

## Supporting Information

# Target-Activated Multicolor Fluorescent Dyes for 3D Imaging of the Plasma Membrane and Tracking of Apoptosis

Junjun Pan,<sup>†a</sup> Xin Peng, <sup>†a</sup> Chuangye Yao,<sup>a</sup> Jiaqi Zuo,<sup>a</sup> Tingting Lei,<sup>b</sup> Hui Feng,<sup>a</sup> Kewei Zhang,<sup>b</sup> Engao Zhu<sup>b\*</sup> and Zhaosheng Qian<sup>a\*</sup>

<sup>a</sup>Key Laboratory of the Ministry of Education for Advanced Catalysis Materials, College of Chemistry and Materials Science, Zhejiang Normal University, Jinhua 321004, China

<sup>b</sup>College of Life Sciences, Zhejiang Normal University, Jinhua 321004, China

## Table of Contents

### 1. Synthesis and Characterization of Dyes

### 2. Experimental Protocols for Optical Characterization and Confocal Imaging

- 2.1 Characterization of UV-Visible and Fluorescence Properties of All Samples
- 2.2 Fluorescence Turn-on Assay of SD Dyes to DOPC
- 2.3 Toxicity Test of Fluorescent Dyes towards *Arabidopsis Thaliana*
- 2.4 Confocal Imaging of Plasma Membrane of Onion Epidermal Cells
- 2.5 Long-term Imaging of Plasma Membrane of Onion Epidermal Cells
- 2.6 Dynamic Monitoring of Calcium-Mediated Apoptosis of Onion Epidermal Cells

Dynamic monitoring of calcium-mediated apoptosis of onion epidermal cells were conducted as follows. A piece of onion internal epidermis from fresh onion was incubated in a 2 mL of MS culture containing SPD-R (5.0  $\mu$ M) for 2 min, and then this piece of onion internal epidermis was placed in a solution of calcium chloride (0.5 M) for continuous 70 minutes. At various time points, the onion epidermal cells were observed and recorded on a confocal laser scanning microscope under the optimal conditions.

- 2.7 Three-dimensional Imaging of Plasma Membrane of Onion Epidermal Cells

### 3. Supplementary Schemes and Figures

**Scheme S1.** Synthesis routes of SP-G, SQ-O, SP-R, SQ-NIR.

**Scheme S2.** Synthesis routes of SPD-G, SQD-O, SPD-R, SQD-NIR.

**Table S1.** Spectroscopic properties of SD Dyes.

**Figure S1.** Normalized UV-visible spectra of SP-G, SQ-O, SP-R, SQ-NIR (30.0  $\mu\text{M}$ ) in water.

**Figure S2.** Normalized PL emission spectra of SP-G, SQ-O, SP-R, SQ-NIR (10.0  $\mu\text{M}$ ) in water.

**Figure S3.** Time-resolved PL decay curves of SP-G (a), SQ-O (b), SP-R (c), SQ-NIR (d) in dispersed in adamantane.

**Figure S4.** Time-resolved PL decay curves of SPD-G (a), SQD-O (b), SPD-R (c), SQD-NIR (d) in dispersed in adamantane.

**Figure S5.** PL spectra of SPD-G (a) (10.0 nM), SQD-O (b) (10.0 nM), SPD-R (c) (5.0  $\mu\text{M}$ ), SQD-NIR (d) (10.0  $\mu\text{M}$ ) in  $\text{H}_2\text{O}$  and in DOPC solution (5 mg/mL).

**Figure S6.** Laser scanning confocal microscopy images of onion epidermal cells stained with different amounts of dyes at different staining time. (A) SPD-G for 10 min: (a, d) 5.0  $\mu\text{M}$ ; (b, e) 10.0  $\mu\text{M}$ ; (c, f) 20.0  $\mu\text{M}$ ; (B) SQD-O for 15 min: (a, d) 10.0  $\mu\text{M}$ ; (b, e) 20.0  $\mu\text{M}$ ; (c, f) 30.0  $\mu\text{M}$ ; (C) SPD-R for 2 min: (a, d) 1.0  $\mu\text{M}$ ; (b, e) 5.0  $\mu\text{M}$ ; (c, f) 10.0  $\mu\text{M}$ ; (D) SQD-NIR for 20 min: (a, d) 5.0  $\mu\text{M}$ ; (b, e) 10.0  $\mu\text{M}$ ; (c, f) 20.0  $\mu\text{M}$ .

**Figure S7.** Laser scanning confocal microscopy images of onion epidermal cells stained with different amounts of dyes at different staining time. (A) SP-G for 15 min: (a, d) 10.0  $\mu\text{M}$ ; (b, e) 20.0  $\mu\text{M}$ ; (c, f) 30.0  $\mu\text{M}$ ; (B) SQ-O for 15 min: (a, d) 20.0  $\mu\text{M}$ ; (b, e) 30.0  $\mu\text{M}$ ; (c, f) 40.0  $\mu\text{M}$ ; (C) SP-R for 2 min: (a, d) 1.0  $\mu\text{M}$ ; (b, e) 5.0  $\mu\text{M}$ ; (c, f) 10.0  $\mu\text{M}$ ; (D) SQ-NIR for 20 min: (a, d) 10.0  $\mu\text{M}$ ; (b, e) 20.0  $\mu\text{M}$ ; (c, f) 30.0  $\mu\text{M}$ .

**Figure S8.** Laser scanning confocal microscopy images of onion epidermal cells stained with different control dyes after plasmolysis using a NaCl solution. Plasmolysis was achieved using a NaCl solution of 0.025 g/mL. (a, e) SP-G (50.0  $\mu\text{M}$ , 10 min); (b, f) SQ-O (50.0  $\mu\text{M}$ , 10 min); (c, g) SP-R (10.0  $\mu\text{M}$ , 10 min); (d, h) SQ-NIR (20.0  $\mu\text{M}$ , 10 min). Scale bar = 50  $\mu\text{m}$ .

**Figure S9.** (a) Photographs of representative *arabidopsis thaliana* seedlings incubated without (Mock) and with different concentrations of SPD-G, SQD-O, SPD-R, SQD-NIR (1.0  $\mu\text{M}$  to 50.0  $\mu\text{M}$ ) after 6 days. (b) Average root lengths of *arabidopsis thaliana* seedlings incubated without (Mock) and with different concentrations of SPD-G, SQD-O, SPD-R, SQD-NIR (1.0  $\mu\text{M}$  to 50.0  $\mu\text{M}$ ) after 6 days.

**Figure S10.** The changes of laser scanning confocal microscopy images of onion epidermal cells stained with SPD-R (5.0  $\mu\text{M}$ ) for 2 min versus irradiation time at 561 nm using the excitation source of the used microscope: (a) 0 min; (b) 10 min; (c) 20 min; (d) 30 min; (e) 40 min; (f) 50 min; (g) 60 min; (h) 70 min; (i) 80 min; (j) 90 min; (k) 100 min; (l) 110 min; (m) 120 min; (n) 130 min. Scale bar = 10  $\mu\text{m}$ . (B) The change

of PL intensity of SPD-R inside the cell membranes versus irradiation time at 561 nm using the excitation source of the used microscope.

**Figure S11.** Laser scanning confocal microscopy images of onion epidermal cells stained with SPD-R (5.0  $\mu$ M) before (a, c) and after treatment of DMSO (b, d). Scale bar = 100  $\mu$ m.

**Figure S12.** Laser scanning confocal microscopy images of onion epidermal cells stained with SP-R (10.0  $\mu$ M) at various time points: (a, g) 0 min; (b, h) 2 min; (c, i) 5 min; (d, j) 10 min; (e, k) 15 min; (f, l) 20 min. Scale bar = 50  $\mu$ m.

**Figure S13.** Laser scanning confocal microscopy images in onion epidermal cells stained with FM 4-64 (5.0  $\mu$ M) at various time points: (a, f) 0 min; (b, g) 5 min; (c, h) 10 min; (d, i) 15min; (e, j) 20min; (p, k) 25 min; (l, q) 30 min; (m, r) 35 min; (n, s) 40 min; (o, t) 45 min. The staining of a portion of nucleus membrane and vacuole membrane were highlighted. Scale bar = 50  $\mu$ m.

**Figure S14.** The average values of  $f_{\text{Signal}}/f_{\text{Background}}$  for onion epidermal cells stained with different SD dyes in 3D images.

#### 4. Spectra of Compounds

**Figure S15.**  $^1\text{H}$  NMR spectra of 1,4-Dimethylpyridine bromide in DMSO

**Figure S16.**  $^{13}\text{C}$  NMR spectra of 1,4-Dimethylpyridine bromide in DMSO

**Figure S17.**  $^1\text{H}$  NMR spectra of 1,4-Dimethylquinolinium bromide in DMSO

**Figure S18.**  $^{13}\text{C}$  NMR spectra of 1,4-Dimethylpyridine bromide in DMSO

**Figure S19.**  $^1\text{H}$  NMR spectra of 4-(4-ethoxystyryl)-1-methyl-pyridinium bromide (SP-G) in DMSO

**Figure S20.**  $^{13}\text{C}$  NMR spectra of 4-(4-ethoxystyryl)-1-methyl-pyridinium bromide (SP-G) in DMSO

**Figure S21.**  $^1\text{H}$  NMR spectra of 4-(4-ethoxystyryl)-1-methyl-quinolinium bromide (SQ-O) in DMSO

**Figure S22.**  $^{13}\text{C}$  NMR spectra of 4-(4-ethoxystyryl)-1-methyl-quinolinium bromide (SQ-O) in DMSO

**Figure S23.**  $^1\text{H}$  NMR spectra of 4-[4-(N,N-diethylamino)styryl]-1-methyl-pyridinium bromide (SP-R) in DMSO

**Figure S24.**  $^{13}\text{C}$  NMR spectra of 4-[4-(N,N-diethylamino)styryl]-1-methyl-pyridinium bromide (SP-R) in DMSO

**Figure S25.**  $^1\text{H}$  NMR spectra of 4-[4-(N,N-diethylamino)styryl]-1-methyl-quinolinium bromide (SQ-NIR) in DMSO

**Figure S26.**  $^{13}\text{C}$  NMR spectra of 4-[4-(N,N-diethylamino)styryl]-1-methyl-quinolinium bromide (SQ-NIR) in DMSO

**Figure S27.**  $^1\text{H}$  NMR spectra of 4-(hexyloxy)benzaldehyde in  $\text{CDCl}_3$

**Figure S28.**  $^{13}\text{C}$  NMR spectra of 4-(hexyloxy)benzaldehyde in  $\text{CDCl}_3$

**Figure S29.**  $^1\text{H}$  NMR spectra of N,N-dihexylaniline in  $\text{CDCl}_3$

**Figure S30.**  $^{13}\text{C}$  NMR spectra of N,N-dihexylaniline in  $\text{CDCl}_3$

**Figure S31.**  $^1\text{H}$  NMR spectra of 4-(dihexylamino)benzaldehyde in  $\text{CDCl}_3$

**Figure S32.**  $^{13}\text{C}$  NMR spectra of 4-(dihexylamino)benzaldehyde in  $\text{CDCl}_3$

**Figure S33.**  $^1\text{H}$  NMR spectra of 1-(3-(3-bromopropyl)-1,4-diazabicyclo[2.2.2]octan-1-ium bromide in  $\text{D}_2\text{O}$

**Figure S34.**  $^{13}\text{C}$  NMR spectra of 1-(3-(3-bromopropyl)-1,4-diazabicyclo[2.2.2]octan-1-ium bromide in  $\text{D}_2\text{O}$

**Figure S35.**  $^1\text{H}$  NMR spectra of 1-(3-(4-methylpyridin-1-ium-1-yl)propyl)-1,4-diazabicyclo[2.2.2]octan-1-ium dibromide in  $\text{D}_2\text{O}$

**Figure S36.**  $^{13}\text{C}$  NMR spectra of 1-(3-(4-methylpyridin-1-ium-1-yl)propyl)-1,4-diazabicyclo[2.2.2]octan-1-ium dibromide in DMSO

**Figure S37.**  $^1\text{H}$  NMR spectra of 1-(3-(4-methylquinolin-1-ium-1-yl)propyl)-1,4-diazabicyclo[2.2.2]octan-1-ium dibromide in DMSO

**Figure S38.**  $^{13}\text{C}$  NMR spectra of 1-(3-(4-methylquinolin-1-ium-1-yl)propyl)-1,4-diazabicyclo[2.2.2]octan-1-ium dibromide in DMSO

**Figure S39.**  $^1\text{H}$  NMR spectra of 1-(3-(4-(4-(hexyloxy)styryl)pyridin-1-ium-1-yl)propyl)-1,4-diazabicyclo[2.2.2]octan-1-ium dibromide (SPD-G) in DMSO

**Figure S40.**  $^{13}\text{C}$  NMR spectra of 1-(3-(4-(4-(hexyloxy)styryl)pyridin-1-ium-1-yl)propyl)-1,4-diazabicyclo[2.2.2]octan-1-ium dibromide (SPD-G) in DMSO

**Figure S41.**  $^1\text{H}$  NMR spectra of 1-(3-(4-(4-(dihexylamino)styryl)quinolin-1-ium-1-yl)propyl)-1,4-diazabicyclo[2.2.2]octan-1-ium dibromide (SQD-O) in DMSO

**Figure S42.**  $^1\text{H}$  NMR spectra of 1-(3-(4-(4-(hexyloxy)styryl)pyridin-1-ium-1-yl)propyl)-1,4-diazabicyclo[2.2.2]octan-1-ium dibromide (SPD-R) in DMSO

**Figure S43.**  $^{13}\text{C}$  NMR spectra of 1-(3-(4-(4-(hexyloxy)styryl)pyridin-1-ium-1-yl)propyl)-1,4-diazabicyclo[2.2.2]octan-1-ium dibromide (SPD-R) SQD-NIR in DMSO

**Figure S44.**  $^1\text{H}$  NMR spectra of 1-(3-(4-(4-(dihexylamino)styryl)quinolin-1-ium-1-yl)propyl)-1,4-diazabicyclo[2.2.2]octan-1-ium bromide (SQD-NIR) in DMSO

**Figure S45.** High-resolution mass spectrum of 1,4-Dimethylpyridine bromide

**Figure S46.** High-resolution mass spectrum of 1,4-Dimethylquinolinium bromide

**Figure S47.** High-resolution mass spectrum of 4-(4-ethoxystyryl)-1-methyl-pyridinium bromide (SP-G)

**Figure S48.** High-resolution mass spectrum of 4-(4-ethoxystyryl)-1-methyl-quinolinium bromide (SQ-O)

**Figure S49.** High-resolution mass spectrum of 4-[4-(N,N-diethylamino)styryl]-1-methyl-pyridinium bromide (SP-R)

**Figure S50.** High-resolution mass spectrum of 4-[4-(N,N-diethylamino)styryl]-1-methyl-quinolinium bromide (SQ-NIR)

**Figure S51.** High-resolution mass spectrum of 4-(hexyloxy)benzaldehyde

**Figure S52.** High-resolution mass spectrum of N,N-dihexylaniline

**Figure S53.** High-resolution mass spectrum of 4-(dihexylamino)benzaldehyde

**Figure S54.** High-resolution mass spectrum of 1-(3-bromopropyl)-1,4-diazabicyclo[2.2.2]octan-1-ium bromide

**Figure S55.** High-resolution mass spectrum of 1-(3-(4-methylpyridin-1-ium-1-yl)propyl)-1,4-diazabicyclo[2.2.2]octan-1-ium dibromide

**Figure S56.** High-resolution mass spectrum of 1-(3-(4-methylquinolin-1-ium-1-yl)propyl)-1,4-diazabicyclo[2.2.2]octan-1-ium dibromide.

**Figure S57.** High-resolution mass spectrum of 1-(3-(4-(4-(hexyloxy)styryl)pyridin-1-ium-1-yl)propyl)-1,4-diazabicyclo[2.2.2]octan-1-ium dibromide (SPD-G)

**Figure S58.** High-resolution mass spectrum of 1-(3-(4-(4-(dihexylamino)styryl)quinolin-1-ium-1-yl)propyl)-1,4-diazabicyclo[2.2.2]octan-1-ium dibromide (SQD-O)

**Figure S59.** High-resolution mass spectrum of 1-(3-(4-(4-(hexyloxy)styryl)pyridin-1-ium-1-yl)propyl)-1,4-diazabicyclo[2.2.2]octan-1-ium dibromide (SPD-R)

**Figure S60.** High-resolution mass spectrum of 1-(3-(4-(4-(dihexylamino)styryl)quinolin-1-ium-1-yl)propyl)-1,4-diazabicyclo[2.2.2]octan-1-ium bromide (SQD-NIR)

## 1. Synthesis and Characterization of Dyes

**Synthesis of 1,4-dimethylpyridinium bromide.** 4-Methylpyridine (1.86 g, 20 mmol) was added to 20 mL of acetonitrile in a 50 mL two necked flask, and then bromomethane (2.37 g, 25 mmol) was added. The mixture was refluxed for 12 h. After cooling to room temperature, a large amount of precipitates as a solid were obtained. The crude product was washed several times with ethyl acetate, and then removal of the solvent under reduced pressure to give 1,4-dimethylpyridinium bromide as a white solid (3.02 g, 80%). Molecular formula: C<sub>7</sub>H<sub>10</sub>BrN. <sup>1</sup>H NMR (400 MHz, DMSO) δ 8.79 (d, *J* = 6.0 Hz, 2H), 7.94 (d, *J* = 6.1 Hz, 2H), 4.26 (s, 3H), 2.59 (s, 3H). <sup>13</sup>C NMR (101 MHz, DMSO) δ 158.75, 144.99, 128.45, 47.58, 21.76. HRMS (*m/z*): calcd. for C<sub>7</sub>H<sub>10</sub>BrN [M-Br]<sup>+</sup>108.0808, found 108.0808.

**Synthesis of 1,4-dimethylquinolinium bromide.** 4-Methylquinoline (2.86 g, 20 mmol) was added to 20 mL of 1,4-dioxane in a 50 mL two necked flask, and then bromomethane (2.37 g, 25 mmol) was added. The mixture was refluxed for 12 h. After cooling to room temperature, a large amount of precipitates as a solid were obtained. The crude product was washed several times with ethyl acetate, and then removal of the solvent under reduced pressure to give 1,4-dimethylquinolinium bromide as a light yellow solid (3.95 g, 83%). Molecular formula: C<sub>11</sub>H<sub>12</sub>BrN. <sup>1</sup>H NMR (400 MHz, DMSO) δ 9.32 (d, *J* = 6.0 Hz, 1H), 8.53 (d, *J* = 8.4 Hz, 1H), 8.47 (d, *J* = 8.9 Hz, 1H), 8.26 (t, *J* = 7.9 Hz, 1H), 8.07 (d, *J* = 7.6 Hz, 1H), 8.03 (d, *J* = 6.5 Hz, 1H), 4.57 (s, 3H), 3.00 (s, 3H). <sup>13</sup>C NMR (101 MHz, DMSO) δ 158.70, 149.42, 138.17, 135.41, 130.12, 128.96, 127.24, 122.91, 119.94, 45.43, 20.01. HRMS (*m/z*): calcd. for C<sub>11</sub>H<sub>12</sub>BrN [M-Br]<sup>+</sup> 158.0965, found 158.0964.

**Synthesis of 4-(4-ethoxystyryl)-1-methyl-pyridinium bromide (SP-G).** A mixture of 1,4-dimethylpyridinium bromide (1.88 g, 10 mmol), 4-methoxybenzaldehyde (2.25 g, 15 mmol) and pyrrolidine (20 drops) were stirred overnight in 30 ml of ethanol. The precipitate was then filtered out and washed with ethanol to remove unreacted reactants. The precipitate was dried to give the final product as a hygroscopic yellow solid (2.79 g, 87%). Molecular formula: C<sub>16</sub>H<sub>18</sub>BrNO. <sup>1</sup>H NMR (400 MHz, DMSO) δ 8.77 (d, *J* = 6.2 Hz, 2H), 8.13 (d, *J* = 6.2 Hz, 2H), 7.94 (d, *J* = 16.3 Hz,

1H), 7.70 (d,  $J = 8.1$  Hz, 2H), 7.33 (d,  $J = 16.3$  Hz, 1H), 7.04 (d,  $J = 8.1$  Hz, 2H), 4.22 (s, 3H), 4.10 (q, 2H), 1.35 (t,  $J = 6.9$  Hz, 3H).  $^{13}\text{C}$  NMR (101 MHz, DMSO)  $\delta$  161.00, 153.35, 145.34, 141.10, 130.47, 128.09, 123.47, 121.10, 115.53, 63.87, 47.20, 15.03. HRMS (m/z): calcd. for  $\text{C}_{16}\text{H}_{18}\text{BrNO}$  [M-Br] $^{+}$  240.1383, found 240.1382.

**Synthesis of 4-(4-ethoxystyryl)-1-methyl-quinolinium bromide (SQ-O).** A mixture of 1,4-dimethylquinolinium bromide (2.38 g, 10 mmol), 4-ethoxybenzaldehyde (2.25 g, 15 mmol) and pyrrolidine (20 drops) were stirred overnight in 30 ml of ethanol. The precipitate was then filtered out and washed with ethanol to remove unreacted reactants. The precipitate was dried to give the final product as a hygroscopic orange solid (1.67 g, 45%). Molecular formula:  $\text{C}_{20}\text{H}_{20}\text{BrNO}$ .  $^1\text{H}$  NMR (400 MHz, DMSO)  $\delta$  9.27 (d,  $J = 6.6$  Hz, 1H), 9.04 (d,  $J = 8.1$  Hz, 1H), 8.43 (d,  $J = 6.5$  Hz, 2H), 8.25 (t,  $J = 8.4$  Hz, 1H), 8.16 (d,  $J = 4.5$  Hz, 2H), 8.02 (t,  $J = 7.7$  Hz, 1H), 7.95 (d,  $J = 8.8$  Hz, 2H), 7.07 (d,  $J = 8.8$  Hz, 2H), 4.51 (s, 3H), 4.13 (q, 2H), 1.37 (t,  $J = 7.0$  Hz, 3H).  $^{13}\text{C}$  NMR (101 MHz, DMSO)  $\delta$  161.34, 153.39, 148.24, 143.49, 139.23, 135.38, 131.37, 129.55, 128.55, 126.91, 126.65, 119.73, 117.51, 115.96, 115.44, 63.94, 45.04, 15.03. HRMS (m/z): calcd. for  $\text{C}_{20}\text{H}_{20}\text{BrNO}$  [M-Br] $^{+}$ : 290.1540, found: 290.1539.

**Synthesis of 4-[4-(*N,N*-diethylamino)styryl]-1-methyl-pyridinium bromide (SP-R).** A mixture of 1,4-dimethylpyridinium bromide (1.88 g, 10 mmol), 4-(*N,N*-diethylamino)benzaldehyde (2.66 g, 15 mmol) and pyrrolidine (20 drops) were stirred overnight in 30 ml of ethanol. The precipitate was then filtered out and washed with ethanol to remove unreacted reactants. The precipitate was dried to give the final product as a hygroscopic dark red solid (2.70 g, 78%). Molecular formula:  $\text{C}_{18}\text{H}_{23}\text{BrN}_2$ .  $^1\text{H}$  NMR (400 MHz, DMSO)  $\delta$  8.64 (d,  $J = 6.4$  Hz, 2H), 8.01 (d,  $J = 6.4$  Hz, 2H), 7.87 (d,  $J = 16.0$  Hz, 1H), 7.56 (d,  $J = 8.6$  Hz, 2H), 7.11 (d,  $J = 16.1$  Hz, 1H), 6.74 (d,  $J = 8.6$  Hz, 2H), 4.16 (s, 3H), 3.42 (q, 4H), 1.12 (t,  $J = 6.9$  Hz, 6H).  $^{13}\text{C}$  NMR (101 MHz, DMSO)  $\delta$  153.89, 149.94, 144.70, 142.45, 131.03, 122.43, 122.18, 116.94, 111.85, 46.75, 44.33, 12.96. HRMS (m/z): calcd. for  $\text{C}_{18}\text{H}_{23}\text{BrN}_2$  [M-Br] $^{+}$  267.1856, found 267.1853.

**Synthesis of 4-[4-(*N,N*-diethylamino)styryl]-1-methyl-quinolinium bromide (SQ-NIR).** A mixture of 1,4-dimethylquinolinium bromide (2.38 g, 10 mmol), 4-(*N,N*-diethylamino)benzaldehyde

(2.66 g, 15 mmol) and pyrrolidine (20 drops) were stirred overnight in 30 ml of ethanol. The precipitate was then filtered out and washed with ethanol to remove unreacted reactants. The precipitate was dried to give the final product as a hygroscopic deep purple solid (2.78 g, 70%). Molecular formula:  $C_{22}H_{25}BrN_2$ .  $^1H$  NMR (400 MHz, DMSO)  $\delta$  9.04 (d,  $J$  = 6.5 Hz, 1H), 8.99 (d,  $J$  = 8.5 Hz, 1H), 8.30 (t,  $J$  = 6.8 Hz, 2H), 8.19 (d,  $J$  = 7.4 Hz, 1H), 8.14 (d,  $J$  = 15.8 Hz, 1H), 7.95 (t,  $J$  = 6.8 Hz, 2H), 7.83 (d,  $J$  = 8.5 Hz, 2H), 6.79 (d,  $J$  = 8.5 Hz, 2H), 4.42 (s, 3H), 3.47 (q, 4H), 1.15 (t,  $J$  = 6.8 Hz, 6H).  $^{13}C$  NMR (101 MHz, DMSO)  $\delta$  153.64, 150.49, 147.06, 145.22, 139.26, 135.02, 132.25, 128.94, 126.72, 126.15, 122.91, 119.42, 114.12, 112.95, 111.90, 44.44, 44.35, 12.98. HRMS (m/z): calcd. for  $C_{22}H_{25}BrN_2$  [M-Br] $^+$  317.2013, found 317.2013.

**Synthesis of 4-hexyloxybenzaldehyde.** 4-Hydroxybenzaldehyde (2.5 g, 20 mmol) was added to 30 mL of DMF in a 50 mL two necked flask, and then 1-bromohexane (2.5 g, 15 mmol) and  $K_2CO_3$  (4.1 g, 30 mmol) were added into the aforementioned solution. The mixture was refluxed for 12 h. After cooling to room temperature, the mixture was poured into water, and then the product was extracted with petroleum ether. The organic layer was washed with water 3 times (3 $\times$ 50 mL) and then dried by anhydrous  $Na_2SO_4$ . The solvent was removed by rotary evaporation to give a light yellow liquid of 4-hexyloxybenzaldehyde (2.60 g, 84%). Molecular formula:  $C_{13}H_{18}O_2$ .  $^1H$  NMR (600 MHz,  $CDCl_3$ )  $\delta$  9.87 (s, 1H), 7.82 (d,  $J$  = 8.8 Hz, 2H), 6.98 (d,  $J$  = 8.7 Hz, 2H), 4.03 (t,  $J$  = 6.6 Hz, 2H), 1.84 – 1.77 (m, 2H), 1.50 – 1.43 (m, 2H), 1.36 – 1.33 (m, 4H), 0.91 (t,  $J$  = 7.1 Hz, 3H).  $^{13}C$  NMR (151 MHz,  $CDCl_3$ )  $\delta$  190.82, 164.27, 131.99, 129.73, 114.74, 68.43, 31.53, 29.03, 25.64, 22.59, 14.03. HRMS (m/z): calcd. for  $C_{13}H_{18}O_2$  [M+H] $^+$  207.1385, found 207.1379.

**Synthesis of N,N-dihexylaniline.** Aniline (1.4 g, 15 mmol) was added to 30 mL of DMF in a 50 mL two necked flask, and then 1-bromohexane (8.7 g, 53 mmol),  $K_2CO_3$  (8.7 g, 63 mmol) and KI (3.7 g, 22 mmol) were added into the aforementioned solution. The mixture was stirred at 120  $^{\circ}C$  for 7 h. After cooling to room temperature, the resulting solution was filtered to remove the precipitate. The filtrate was poured into water. and then the product was extracted with DCM. The organic layer was washed with water 3 times (3 $\times$ 50 mL) and dried by anhydrous  $Na_2SO_4$ . The



solvent was removed by rotary evaporation. The crude product was purified by column chromatography to give a light yellow liquid. (3.30 g, 85%). Molecular formula: C<sub>18</sub>H<sub>31</sub>N. <sup>1</sup>H NMR (400 MHz, CDCl<sub>3</sub>) δ 7.28 – 7.19 (m, 2H), 6.69 – 6.64 (m, 7.6 Hz, 3H), 3.29 (t, *J* = 6.7 Hz, 4H), 1.63 – 1.58 (m, 4H), 1.40 – 1.33 (m, 12H), 0.94 (t, *J* = 6.7 Hz, 6H). <sup>13</sup>C NMR (101 MHz, CDCl<sub>3</sub>) δ 148.17, 129.22, 115.02, 111.63, 51.08, 31.81, 27.23, 26.92, 22.76, 14.12. HRMS (*m/z*): calcd. for C<sub>18</sub>H<sub>31</sub>N [M+H]<sup>+</sup> 262.2535, found 262.2557.

**Synthesis of 4-(N,N-dihexylamino)benzaldehyde.** N,N-Dihexylaniline (2.0 g, 7.65 mmol) was added into 30 mL of DMF in a 50 ml round bottom flask, and then POCl<sub>3</sub> (2.0 g, 13.23 mmol) was slowly added under an ice bath. The resulting mixture was stirred at 120 °C for 7 hours during which a brown precipitate appeared. After cooling to room temperature, the reaction was quenched by ice water, and then the green solution was stirred for 20 minutes. After that, the mixture was poured into water, and the product was extracted with DCM. The organic layer was washed with water 3 times (3×50 mL) and dried by anhydrous Na<sub>2</sub>SO<sub>4</sub>. All solvents were removed from the system by rotary evaporation. The crude product was obtained by removing the solvent, and then further purified by column chromatography (EA:PE=1:10) to give a brownish liquid (2.1 g, 95%). Molecular formula: C<sub>19</sub>H<sub>31</sub>NO. <sup>1</sup>H NMR (400 MHz, CDCl<sub>3</sub>) δ 9.69 (s, 1H), 7.69 (d, *J* = 8.9 Hz, 2H), 6.63 (d, *J* = 9.0 Hz, 2H), 3.33 (t, *J* = 7.0 Hz, 4H), 1.61 – 1.58 (m, 4H), 1.38 – 1.27 (m, 12H), 0.90 (t, *J* = 6.7 Hz, 6H). <sup>13</sup>C NMR (151 MHz, CDCl<sub>3</sub>) δ 189.93, 152.59, 132.21, 124.48, 110.65, 51.12, 31.65, 27.12, 26.73, 22.66, 14.04. HRMS (*m/z*): calcd. for C<sub>19</sub>H<sub>31</sub>NO [M+H]<sup>+</sup> 290.2484, found 290.2479.

**Synthesis of 1-(3-bromopropyl)-1,4-diazabicyclo[2.2.2]octan-1-ium bromide.** 1,3-Dibromopropane (5.15 mL, 50 mmol) was added to a solution of 1,4-diazabicyclo[2.2.2]octane (5.6 g, 50 mmol) in 100 mL acetone. White solid precipitated after the solution was stirred at room temperature for 2~3 hours, and then the precipitates were filtered out and washed with acetone. The final product was dried to give a white powder (12.88 g, 82%). Molecular formula: C<sub>9</sub>H<sub>18</sub>Br<sub>2</sub>N<sub>2</sub>. <sup>1</sup>H NMR (400 MHz, D<sub>2</sub>O) δ 3.50 (t, *J* = 8.0 Hz, 2H), 3.46 – 3.38 (m, 8H), 3.15 (t, *J* = 8.0 Hz, 2H), 2.39 – 2.29 (m, 2H). <sup>13</sup>C NMR (101 MHz, D<sub>2</sub>O) δ 63.05, 52.23, 44.10, 28.97, 24.32.

HRMS (m/z): calcd. for  $C_9H_{18}Br_2N_2$   $[M-2Br]^{2+}$  233.0648, found 233.0649.

**Synthesis of 1-(3-(4-methylpyridin-1-ium-1-yl)propyl)-1,4-diazabicyclo[2.2.2]octan-1-ium dibromide.** 4-Methylpyridine (4.66 g, 50 mmol) was added into a solution of 1-(3-bromopropyl)-1,4-diazabicyclo[2.2.2]octan-1-ium bromide (1.57 g, 5 mmol) in 50 ml of ethanol. The resulting mixture was refluxed for 48 h during which the solution gradually turned turbid. After cooling to room temperature, the ethanol was removed by evaporation under reduced pressure. The crude product was then washed with ethyl acetate several times until 4-methylpyridine was removed, which was monitored using thin layer chromatography (EA:PE=1:5). The final product was dried to give a white powder (1.73 g, 85%). Molecular formula:  $C_{15}H_{25}Br_2N_3$ .  $^1H$  NMR (400 MHz,  $D_2O$ )  $\delta$  8.66 (d,  $J$  = 6.3 Hz, 2H), 7.88 (d,  $J$  = 6.5 Hz, 2H), 4.61 (t,  $J$  = 7.6 Hz, 2H), 4.19 – 4.07 (m, 2H), 3.44 – 3.39 (m, 6H), 3.20 – 3.15 (m, 6H), 2.62 (s, 3H), 2.57 – 2.48 (m, 2H).  $^{13}C$  NMR (101 MHz, DMSO)  $\delta$  159.71, 144.41, 128.88, 60.06, 57.32, 52.17, 45.05, 23.81, 21.92. HRMS (m/z): calcd. for  $C_{15}H_{25}Br_2N_3$   $[M-2Br]^{2+}$  123.6019, found 123.6019.

**Synthesis of 1-(3-(4-methylquinolin-1-ium-1-yl)propyl)-1,4-diazabicyclo[2.2.2]octan-1-ium dibromide.** 4-Methylquinoline (7.16 g, 50 mmol) was added into a solution of 1-(3-bromopropyl)-1,4-diazabicyclo[2.2.2]octan-1-ium bromide (1.57 g, 5 mmol) in 50 ml of ethanol. The resulting mixture was refluxed for 48 h during which the solution gradually turned turbid. After cooling to room temperature, the ethanol was removed by evaporation under reduced pressure. The crude product was then washed with ethyl acetate several times until 4-methylpyridine was removed, which was monitored using thin layer chromatography (EA:PE=1:5). The final product was dried to give a white powder (1.83 g, 80%). Molecular formula:  $C_{19}H_{27}Br_2N_3$ .  $^1H$  NMR (400 MHz, DMSO)  $\delta$  9.56 (d,  $J$  = 6.1 Hz, 1H), 8.77 (d,  $J$  = 8.9 Hz, 1H), 8.59 (d,  $J$  = 8.4 Hz, 1H), 8.30 (t,  $J$  = 7.4 Hz, 1H), 8.16 (t,  $J$  = 6.0 Hz, 1H), 8.09 (d,  $J$  = 15.4 Hz, 1H), 5.15 (t,  $J$  = 7.3 Hz, 2H), 3.75 (s, 6H), 3.42 (s, 2H), 3.13 (d,  $J$  = 6.5 Hz, 6H), 3.04 (s, 3H), 2.42 – 2.39 (m, 2H).  $^{13}C$  NMR (101 MHz, DMSO)  $\delta$  147.64, 139.76, 135.58, 134.13, 128.47, 127.73, 126.05, 121.58, 118.30, 58.67, 50.46, 49.51, 43.20, 18.58. HRMS (m/z): calcd. for  $C_{19}H_{27}Br_2N_3$   $[M-2Br]^{2+}$  148.6097, found 148.6097.

**Synthesis of 1-(3-(4-(4-(hexyloxy)styryl)pyridin-1-ium-1-yl)propyl)-1,4-**

**diazabicyclo[2.2.2]octan-1-ium dibromide (SPD-G).** A mixture of 1-(3-(4-methylpyridin-1-ium-1-yl)propyl)-1,4-diazabicyclo[2.2.2]octan-1-ium dibromide (2.03 g, 5 mmol), 4-(hexyloxy)benzaldehyde (1.55 g, 7.5 mmol) and pyrrolidine (10 drops) were stirred overnight in 30 ml of 1-butanol. The precipitate was then filtered out and washed with ethyl acetate and petroleum ether to remove unreacted reactants. The precipitate was transferred to a 50 mL round bottom flask and the residual solvent was removed by evaporation under reduced pressure to give a hygroscopic yellow solid (1.35 g, 46%). Molecular formula:  $C_{28}H_{41}Br_2N_3O$ .  $^1H$  NMR (400 MHz, DMSO)  $\delta$  9.00 (d,  $J = 6.9$  Hz, 2H), 8.25 (d,  $J = 6.9$  Hz, 2H), 8.07 (d,  $J = 16.3$  Hz, 1H), 7.72 (d,  $J = 8.8$  Hz, 2H), 7.42 (d,  $J = 16.3$  Hz, 1H), 7.05 (d,  $J = 8.9$  Hz, 2H), 4.60 (t,  $J = 7.2$  Hz, 2H), 4.03 (t,  $J = 6.5$  Hz, 2H), 3.33 – 3.31 (m, 8H), 3.07 – 3.00 (m, 6H), 2.49 – 2.39 (m, 2H), 1.77 – 1.67 (m, 2H), 1.45 – 1.38 (m, 2H), 1.33 – 1.29 (m, 4H), 0.87 (t,  $J = 7.1$  Hz, 3H).  $^{13}C$  NMR (101 MHz, DMSO)  $\delta$  161.26, 154.16, 144.69, 141.70, 130.61, 128.12, 123.83, 121.07, 115.58, 68.23, 60.12, 56.91, 52.19, 45.09, 31.45, 29.02, 25.62, 23.72, 22.55, 14.40. HRMS (m/z): calcd. for  $C_{28}H_{41}Br_2N_3O$  [M-2Br] $^{2+}$  217.6620, found 217.6619.

**Synthesis of 1-(3-(4-(4-(dihexylamino)styryl)quinolin-1-ium-1-yl)propyl)-1,4-diazabicyclo[2.2.2]octan-1-ium dibromide (SQD-O).** A certain amounts of 1-(3-(4-methylquinolin-1-ium-1-yl)propyl)-1,4-diazabicyclo[2.2.2]octan-1-ium bromide (2.28 g, 5 mmol), 4-(hexyloxy)benzaldehyde (1.55 g, 7.5 mmol) and pyrrolidine (10 drops) were mixed and stirred overnight in 30 ml of 1-butanol. The precipitate was then filtered out and washed with ethyl acetate and petroleum ether to remove unreacted reactants. The precipitate was transferred to a 50 mL round bottom flask and the residual solvent on the surface was removed by evaporation under reduced pressure to give a hygroscopic orange solid (1.38 g, 43%). Molecular formula:  $C_{32}H_{43}Br_2N_3O$ .  $^1H$  NMR (400 MHz, DMSO)  $\delta$  9.48 (d,  $J = 6.7$  Hz, 1H), 9.13 (d,  $J = 8.8$  Hz, 1H), 8.71 (d,  $J = 9.0$  Hz, 1H), 8.59 (d,  $J = 6.8$  Hz, 1H), 8.32 – 8.20 (m, 3H), 8.05 (d,  $J = 8.0$  Hz, 1H), 8.01 (d,  $J = 8.9$  Hz, 2H), 7.09 (d,  $J = 8.9$  Hz, 2H), 5.12 – 5.05 (m, 2H), 4.06 – 4.06 (m, 2H), 3.72 (d,  $J = 4.9$  Hz, 6H), 3.31 (s, 2H), 3.06 (s, 6H), 2.38 (s, 2H), 1.76 – 1.69 (m, 2H), 1.45 – 1.40 (m, 2H), 1.31 (dd,  $J = 7.1, 3.3$  Hz, 4H), 0.88 (t,  $J = 7.1$  Hz, 3H). HRMS (m/z): calcd. for  $C_{32}H_{43}Br_2N_3O$

[M-2Br]<sup>2+</sup> 242.6698, found 242.6702.

**Synthesis of 1-(3-(4-(4-(hexyloxy)styryl)pyridin-1-ium-1-yl)propyl)-1,4-diazabicyclo[2.2.2]octan-1-ium dibromide (SPD-R).** A mixture of 1-(3-(4-methylpyridin-1-ium-1-yl)propyl)-1,4-diazabicyclo[2.2.2]octan-1-ium dibromide (2.03 g, 5 mmol), *N,N*-dihexylaniline (2.17 g, 7.5 mmol) and pyrrolidine (10 drops) were stirred overnight in 30 ml of 1-butanol. The precipitate was then filtered out and washed with ethyl acetate and petroleum ether to remove unreacted reactants. The precipitate was transferred to a 50 mL round bottom flask and then the residual solvent was removed by evaporation under reduced pressure to give a hygroscopic red solid (1.9 g, 56%). Molecular formula: C<sub>35</sub>H<sub>54</sub>Br<sub>2</sub>N<sub>4</sub>. <sup>1</sup>H NMR (600 MHz, DMSO) δ 8.84 (d, *J* = 6.9 Hz, 2H), 8.10 (d, *J* = 6.9 Hz, 2H), 7.97 (d, *J* = 16.0 Hz, 1H), 7.58 (d, *J* = 8.9 Hz, 2H), 7.16 (d, *J* = 16.0 Hz, 1H), 6.71 (d, *J* = 8.9 Hz, 2H), 4.52 (t, *J* = 7.2 Hz, 2H), 4.15 – 4.07 (m, 4H), 3.34 – 3.32 (m, 6H), 3.06 – 3.02 (m, 8H), 2.44 – 2.39 (m, 2H), 1.57 – 1.47 (m, 4H), 1.29 – 1.25 (m, 12H), 0.86 (t, *J* = 6.7 Hz, 6H). <sup>13</sup>C NMR (151 MHz, DMSO) δ 154.62, 150.43, 143.97, 143.05, 131.12, 122.70, 122.18, 116.90, 111.94, 52.30, 52.19, 51.22, 50.56, 45.09, 31.59, 27.31, 26.48, 23.68, 22.60, 14.39. HRMS (*m/z*): calcd. for C<sub>35</sub>H<sub>54</sub>Br<sub>2</sub>N<sub>4</sub> [M-2Br]<sup>2+</sup> 259.2169, found 259.2171.

**Synthesis of 1-(3-(4-(4-(dihexylamino)styryl)quinolin-1-ium-1-yl)propyl)-1,4-diazabicyclo[2.2.2]octan-1-ium bromide (SQD-NIR).** A certain amounts of 1-(3-(4-methylquinolin-1-ium-1-yl)propyl)-1,4-diazabicyclo[2.2.2]octan-1-ium bromide (2.28 g, 5 mmol), *N,N*-dihexylaniline (2.17 g, 7.5 mmol) and pyrrolidine (10 drops) were mixed and stirred overnight in 30 ml of 1-butanol. The precipitate was then filtered out and washed with ethyl acetate and petroleum ether to remove unreacted reactants. The precipitate was transferred to a 50 mL round bottom flask and the residual solvent on the surface was removed by evaporation under reduced pressure to give a hygroscopic deep purple solid (1.4 g, 41%). Molecular formula: C<sub>38</sub>H<sub>56</sub>Br<sub>2</sub>N<sub>4</sub>. <sup>1</sup>H NMR (400 MHz, DMSO) δ 9.19 (d, *J* = 6.8 Hz, 1H), 9.07 (d, *J* = 8.8 Hz, 1H), 8.57 (d, *J* = 8.9 Hz, 1H), 8.42 (d, *J* = 7.1 Hz, 1H), 8.31 – 8.18 (m, 2H), 8.05 – 7.94 (m, 2H), 7.88 (d, *J* = 8.9 Hz, 2H), 6.78 (d, *J* = 9.0 Hz, 2H), 4.97 (t, *J* = 6.9 Hz, 2H), 4.03 (s, 2H), 3.75 – 3.68 (m, 6H), 3.32 – 3.30 (m, 2H), 3.07 (d, *J* = 6.2 Hz, 6H), 2.39 – 2.34 (m, 2H), 1.62 – 1.52 (m, 4H), 1.36 – 1.28 (m,

12H), 0.88 (t,  $J = 6.4$  Hz, 6H).  $^{13}\text{C}$  NMR (151 MHz, DMSO) HRMS ( $m/z$ ): calcd. for  $\text{C}_{38}\text{H}_{56}\text{Br}_2\text{N}_4$   $[\text{M}-2\text{Br}]^{2+}$  284.2247, found 284.2242.

## 2. Experimental Protocols for Optical Characterization and Confocal Imaging

### 2.1 Characterization of UV-Visible and Fluorescence Properties of All Samples

UV-vis absorption spectra were recorded using an Agilent Cary 5000 UV-Vis-NIR spectrophotometer. Steady PL spectra of all samples were performed on an Edinburgh Instruments model FLS980 fluorescence spectrophotometer equipped with a xenon arc lamp using a front face sample holder. Time-resolved fluorescence measurements were conducted with EPL-series lasers.

### 2.2 Fluorescence Turn-on Assay of SD Dyes to DOPC

A solution of 1, 2-dioleoyl-sn-glycero-3-phosphocholine (DOPC) was prepared in triple distilled water (50 mg/mL), and then added to a dye solution with a fixed concentration, resulting in a 5 mg/mL DOPC solution. The fluorescence spectra of the resulting mixtures at the optimum excitation wavelength were recorded by xenon arc lamp.

### 2.3 Toxicity Test of Fluorescent Dyes towards *Arabidopsis Thaliana*

The wild-type (Col-0) seeds of *Arabidopsis thaliana* were surface sterilized and imbibed for 3 days at 4°C in dark and then sown onto 0.5×Murashige & Skoog (MS) 1.5% (w/v) agar plates. Seedlings were vertically grown on plates in a climate-controlled growth room (22/20°C day/night temperature, 16/8 h photoperiod, and 80  $\mu\text{mol}\cdot\text{s}^{-1}\cdot\text{m}^{-2}$  light intensity). The first group of *Arabidopsis thaliana* was grown under the preceding normal conditions. The other five groups of *Arabidopsis thaliana* were grown on 0.5×Murashige & Skoog (MS) 1.5% (w/v) agar plates containing additional SPD-G, SQD-O, SPD-R, SQD-NIR (1  $\mu\text{M}$ , 5  $\mu\text{M}$ , 10  $\mu\text{M}$ , 20  $\mu\text{M}$  and 50  $\mu\text{M}$ ). The resulting phenotype of two groups was recorded using a camera.

### 2.4 Confocal Imaging of Plasma Membrane of Onion Epidermal Cells

The concentration and dyeing time of SD dyes were optimized using the following steps. A piece of onion internal epidermis from fresh onion was placed in a solution of SPD-G with varying concentrations (5.0, 10.0 and 20.0  $\mu\text{M}$ ) for 10 min at 22°C, and then this piece of onion internal epidermis was placed on the slide glass for the following imaging experiments. Fluorescence imaging experiments were performed on a Zeiss LSM 880 model confocal laser scanning microscope (Germany) with an excitation at 561 nm. The same imaging experiments using SQD-O, SPD-R and SQD-NIR were performed, where the concentrations of SQD-O are 10.0, 20.0 and 30.0  $\mu\text{M}$  respectively. The used concentrations for SPD-R are 1.0, 5.0 and 10.0  $\mu\text{M}$  respectively while those are 5.0, 10.0 and 20.0  $\mu\text{M}$  for SQD-NIR. Under optimal conditions, confocal images of onion epidermal cells stained with SPD-G (10.0  $\mu\text{M}$ , 10 min), SQD-O (20.0  $\mu\text{M}$ , 15 min), SPD-R (5.0  $\mu\text{M}$ , 2 min), SQD-NIR (10.0  $\mu\text{M}$ , 20 min) and FM 4-64 (10.0  $\mu\text{M}$ , 2 min) were recorded on a Leica TCS SP5 model confocal laser scanning microscope (Germany) with an excitation at 561 nm. The similar imaging experiments of onion epidermal cells with control dyes were performed using the same procedure. The test concentrations for SP-G are 10.0, 20.0 and 30.0  $\mu\text{M}$  for SP-G with 10 min of staining time while those for SQ-O are 20.0, 30.0 and 40.0  $\mu\text{M}$  for SQ-O with 15 min of staining time. The test concentrations for SP-R are 1.0, 5.0 and 10.0  $\mu\text{M}$  with 2 min of staining time while those for SQ-NIR are 10.0, 20.0 and 30.0  $\mu\text{M}$  with 15 min of staining time.

The photostability of SD dyes was evaluated using fluorescence changes of SPD-R after staining onion epidermal cells. A piece of onion internal epidermis from fresh onion was first stained with SPD-R (5.0  $\mu\text{M}$ ) for 2 min, and then the stained onion epidermal cells were continuous irradiated for 130 min using the light of microscopy light source at 561 nm. The corresponding confocal images were recorded at various time points from 0 min to 130 min with an interval of ten minutes.

Co-localization experiments of cell nuclei stained with SPD-R and DAPI were conducted as follows. A piece of onion internal epidermis from fresh onion was incubated in a 2 mL of MS culture containing 1.0  $\mu\text{g/mL}$  DAPI for 20 min, and then the epidermis was placed on the slide glass before dropping a solution of SPD-R at 5.0  $\mu\text{M}$ . After 2 minutes, the onion epidermal cells

were recorded on a confocal laser scanning microscope using excitation light at different wavelengths of 405 nm and 561 nm respectively.

To evaluate the staining specificity of the dyes to plasma membrane, plasmolysis experiments were conducted as follows. A piece of onion internal epidermis from fresh onion was incubated in a NaCl solution (0.025 g/mL) containing a certain concentration of dyes for a fixed time, during which the staining and plasmolysis were simultaneously achieved. The used concentrations of SPD-G, SQD-O, SPD-R, SQD-NIR and FM 4-64 were 10.0, 20.0, 10.0, 10.0 and 10.0  $\mu\text{M}$  respectively to ensure the image quality, and their staining time was 10 min. The same protocol was also applied to those stained with control dyes. The used concentrations of SP-G, SQ-O, SP-R and SQ-NIR were 50.0, 50.0, 10.0, 10.0 and 20.0  $\mu\text{M}$  respectively to ensure the image quality.

To verify whether the interior of onion epidermal cells can be stained by entered SPD-R dye, the plasma membrane was artificially damaged using DMSO during the staining procedure. A piece of onion internal epidermis from fresh onion was first stained with SPD-R (5.0  $\mu\text{M}$ ) for 2 min, and then the stained onion epidermal cells were placed into a DMSO solution for several seconds to damage the plasma membrane. The onion internal epidermis was placed on the slide glass for the following imaging experiments.

## **2.5 Long-term Imaging of Plasma Membrane of Onion Epidermal Cells**

Long-term imaging experiments of onion epidermal cells were performed according to the following procedure. A piece of onion internal epidermis from fresh onion was incubated in a 2 mL of MS culture containing 5.0  $\mu\text{M}$  SPD-R for 2 min, and then the epidermis was placed between two sealed slide glasses ensuring long-time stability during imaging. Confocal images of onion epidermal cells stained with SPD-R were collected every hour for a total seven consecutive hours under optimal conditions. The similar protocol was applied to long-term imaging experiments using SP-R and FM 4-64 as the stain. The used concentrations for SP-R and FM 4-64 were both 10.0  $\mu\text{M}$ . Confocal images of onion epidermal cells stained with SP-R were collected every five minutes for a total 20 consecutive minutes whereas those stained with FM 4-64 were recorded every ten minutes for a total 40 consecutive minutes.

## 2.6 Dynamic Monitoring of Calcium-Mediated Apoptosis of Onion Epidermal Cells

Dynamic monitoring of calcium-mediated apoptosis of onion epidermal cells were conducted as follows. A piece of onion internal epidermis from fresh onion was incubated in a 2 mL of MS culture containing SPD-R (5.0  $\mu$ M) for 2 min, and then this piece of onion internal epidermis was placed in a solution of calcium chloride (0.5 M) for continuous 70 minutes. At various time points, the onion epidermal cells were observed and recorded on a confocal laser scanning microscope under the optimal conditions.

## 2.7 Three-dimensional Imaging of Plasma Membrane of Onion Epidermal Cells

Three-dimensional imaging of onion epidermal cells was performed as follows. A piece of onion internal epidermis from fresh onion was incubated in a 2 mL of MS culture containing 5.0  $\mu$ M SPD-R for 2 min, and then the epidermis was placed on the slide glass. Confocal images of onion epidermal cells were collected every 1  $\mu$ m from the top to the bottom under the optimal conditions. The three-dimensional images and videos were obtained using the ImageJ software based on all the 2D confocal images. The same protocol was applied to obtain 3D images of plasma membrane after plasmolysis, where the stain solution was replaced with a NaCl solution (0.025 g/mL) containing SPD-R. 3D images of onion epidermal cells stained with SPD-G, SQD-O and SQD-NIR were collected according to the similar protocols under their optimal conditions.

The optical parameters of the dyes used for confocal imaging experiments were summarized as follows.

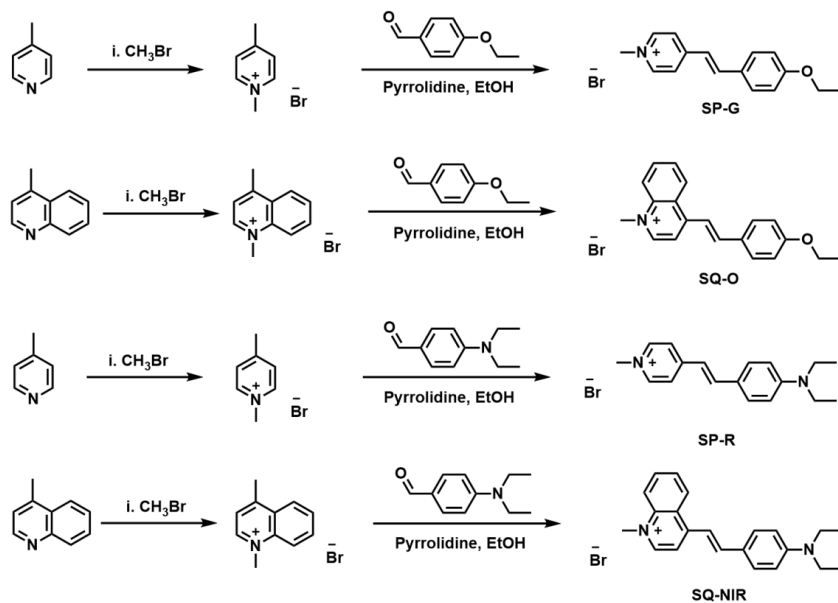
	$\lambda_{\text{ex}}$ (nm)	$\lambda_{\text{em}}$ (nm)
SP-G/SPD-G	405	440-557
SQ-O/SQD-O	405	450-600
SP-R/SPD-R	561	590-661
SQ-NIR/SQD-NIR	561	621-723
FM 4-64	561	592-758
DAPI	405	410-585



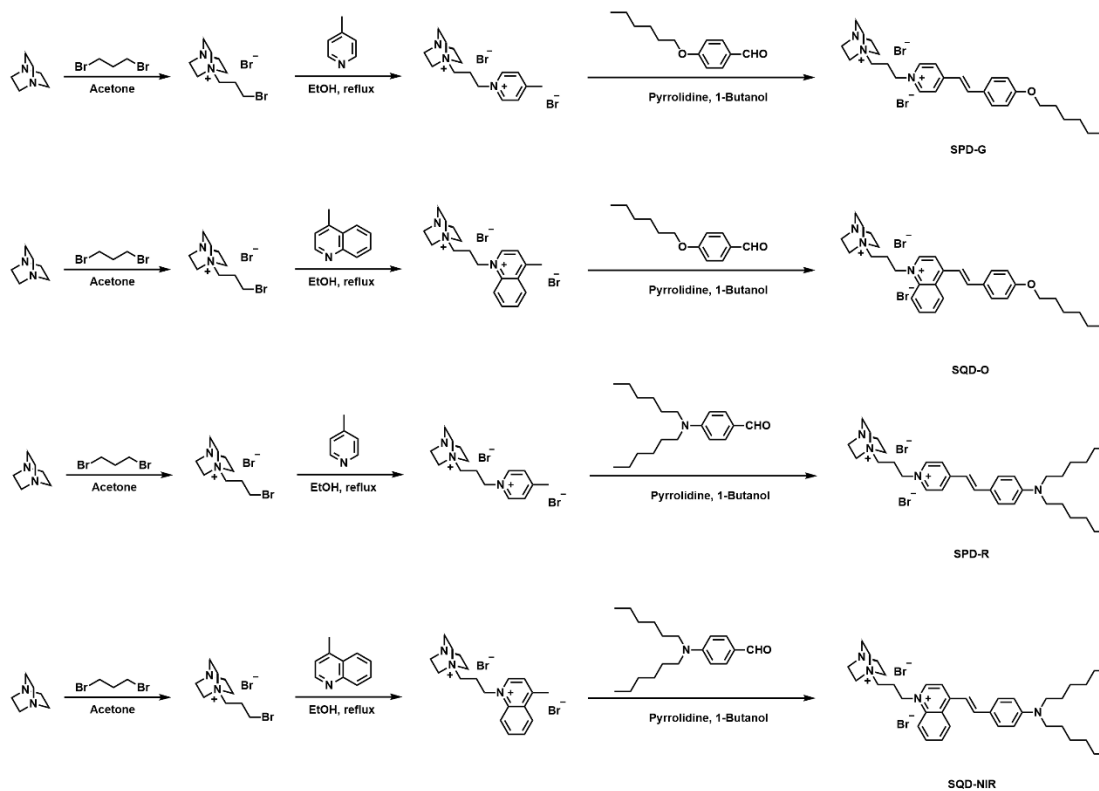
## 2.8 The Statistical Data Process Details of Quantitative Analysis

Data statistics quantified by "ImageJ" software include signal to noise ratio ( $f_{\text{Signal}}/f_{\text{Background}}$ ) of stained plasma membrane, signal ratios of plasma membrane to cell wall ( $f_{\text{cell membrane}}/f_{\text{cell wal}}$ ), Pearson's coefficient, and signal ratio of cell interior ( $S_{\text{Interior signal}}$ ). Signal-to-noise ratio ( $f_{\text{Signal}}/f_{\text{Background}}$ ) of stained plasma membrane: import the merged images into the software, and separate the channels; select the dark field channel and click "Threshold" to calculate the average value (average gray value). For the signal-to-noise ratio of the membrane and the wall ( $f_{\text{cell membrane}}/f_{\text{cell wall}}$ ): select the box tool to select the cell membrane and the cell wall to obtain the mean gray value to calculate the ratio. Pearson coefficient (Pearson's correlation coefficient  $r$ ): import the merged image into the software and separate the channel, use the "JACoP" plugin, and click "Threshold" to calculate the Pearson coefficient. Signal ratio ( $S_{\text{Interior signal}}$ ): the merged images are imported into software and the channel is separated, and the internal cell area is selected to calculate the internal fluorescence signal area of the internal fluorescence area and the internal cell area  $S_{\text{Interior signal}}$ . All the data were obtained using more than 10 samples.

### 3. Supplementary Schemes and Figures



**Scheme S1.** Synthesis routes of SP-G, SQ-O, SP-R, SQ-NIR.



**Scheme S2.** Synthesis routes of SPD-G, SQD-O, SPD-R, SQD-NIR.

**Table S1.** Spectroscopic properties of SD Dyes.

<i>Dyes</i>	$\lambda_{Abs}$ (nm)	$\epsilon * 10^3 (L \cdot mol^{-1} \cdot cm^{-1})$	$\lambda_{Ex}$ (nm)	$\lambda_{Em}$ (nm)	$\Phi(DOPC)$
SPD-G	382	17.15	376	504	0.01
SQD-O	425	2.44	423	564	0.08
SPD-R	496	34.13	464	616	0.67
SQD-NIR	572	13.80	546	678	0.34

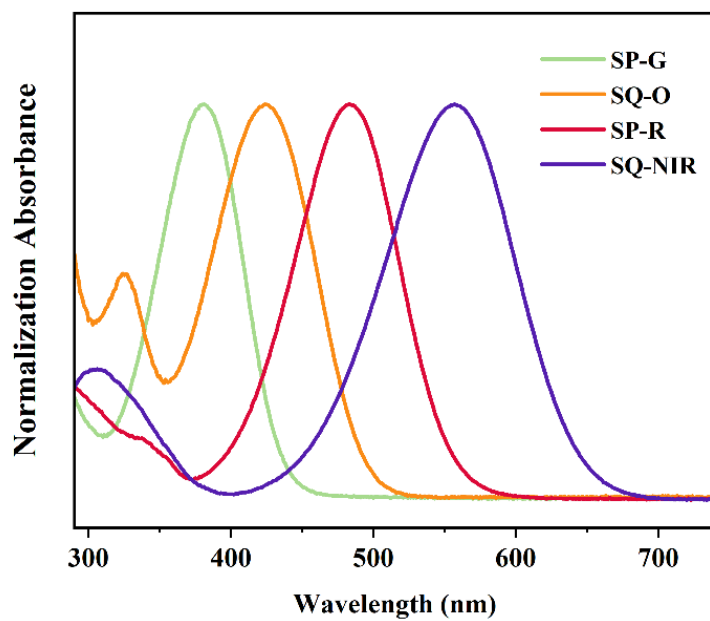


**Figure S1.** Normalized UV-visible spectra of SP-G, SQ-O, SP-R, SQ-NIR (30.0  $\mu$ M) in water.

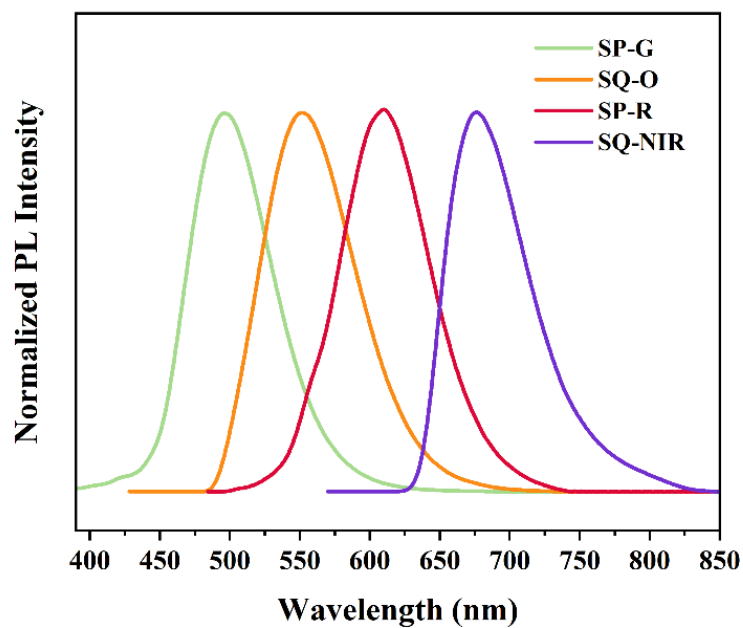


**Figure S2.** Normalized PL emission spectra of SP-G, SQ-O, SP-R, SQ-NIR (10.0  $\mu\text{M}$ ) in water.

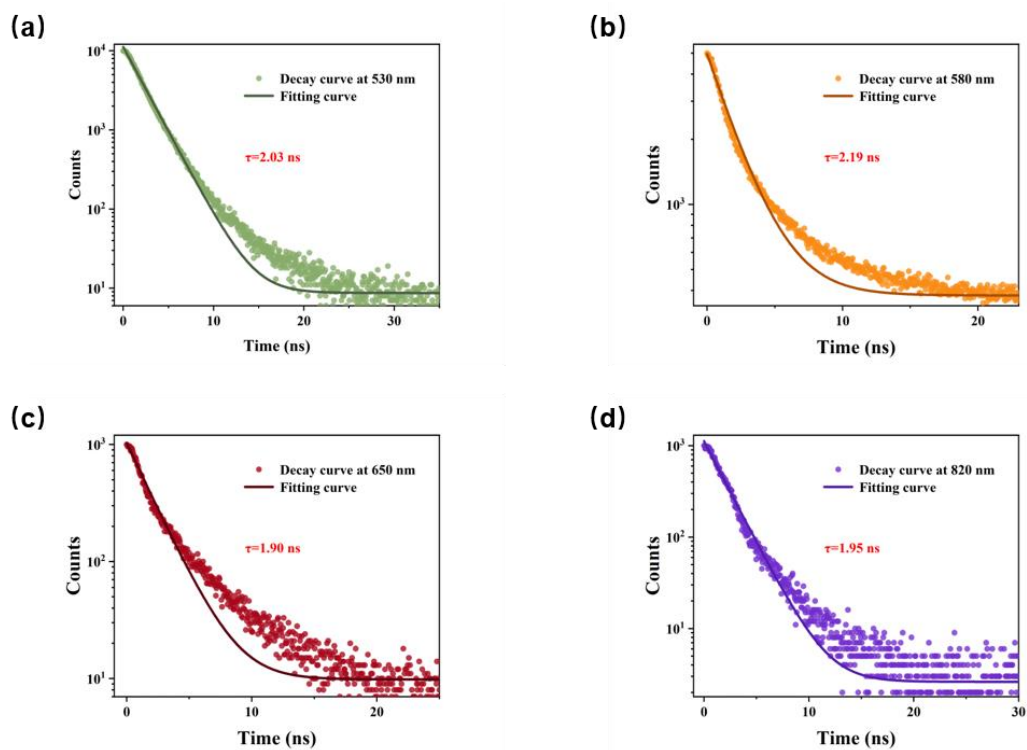


**Figure S3.** Time-resolved PL decay curves of SP-G (a), SQ-O (b), SP-R (c), SQ-NIR (d) in dispersed in adamantane.

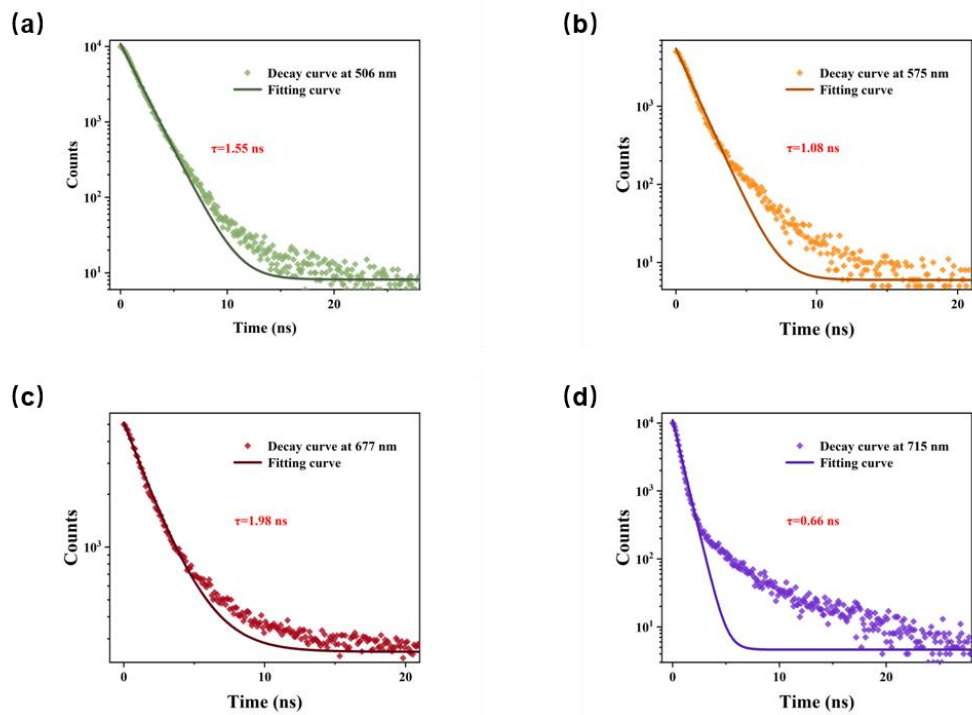


**Figure S4.** Time-resolved PL decay curves of SPD-G (a), SQD-O (b), SPD-R (c), SQD-NIR (d) in dispersed in adamantane.

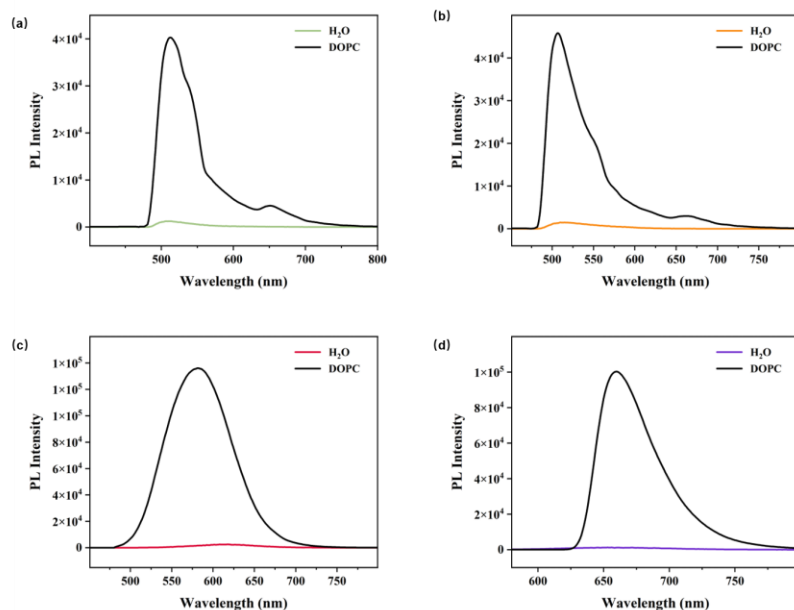


**Figure S5.** PL spectra of SPD-G (a) (10.0 nM), SQD-O (b) (10.0 nM), SPD-R (c) (5.0  $\mu$ M), SQD-NIR (d) (10.0  $\mu$ M) in H<sub>2</sub>O and in DOPC solution (5 mg/mL).

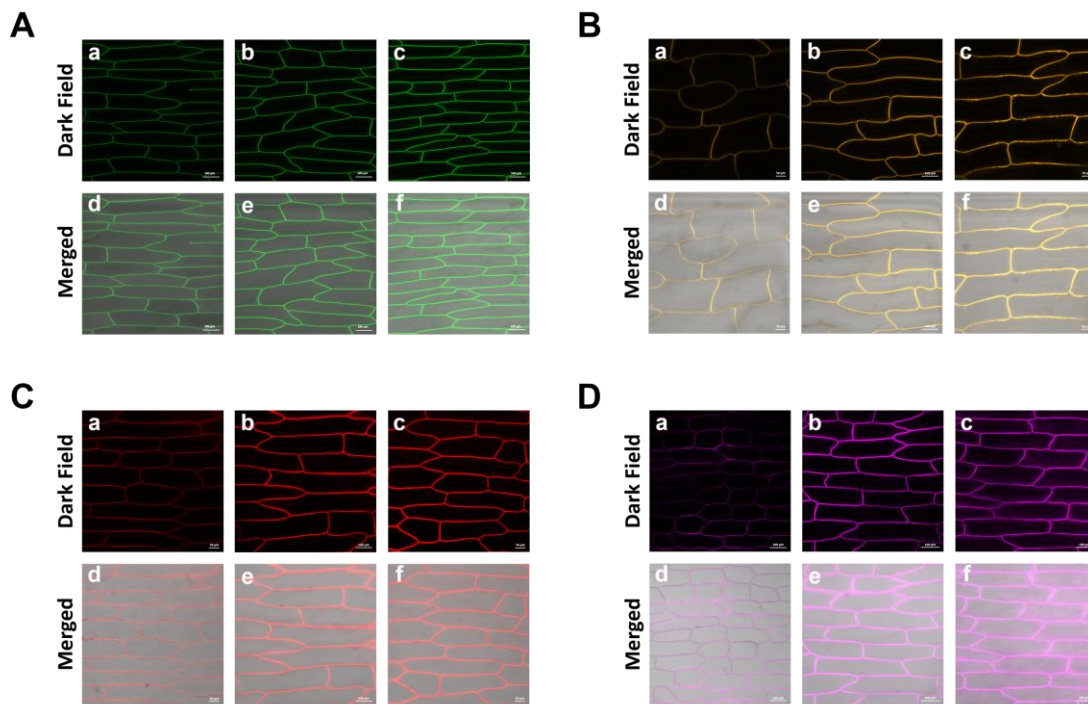


**Figure S6.** Laser scanning confocal microscopy images of onion epidermal cells stained with different amounts of dyes at different staining time. (A) SPD-G for 10 min: (a, d) 5.0  $\mu\text{M}$ ; (b, e) 10.0  $\mu\text{M}$ ; (c, f) 20.0  $\mu\text{M}$ ; (B) SQD-O for 15 min: (a, d) 10.0  $\mu\text{M}$ ; (b, e) 20.0  $\mu\text{M}$ ; (c, f) 30.0  $\mu\text{M}$ ; (C) SPD-R for 2 min: (a, d) 1.0  $\mu\text{M}$ ; (b, e) 5.0  $\mu\text{M}$ ; (c, f) 10.0  $\mu\text{M}$ ; (D) SQD-NIR for 20 min: (a, d) 5.0  $\mu\text{M}$ ; (b, e) 10.0  $\mu\text{M}$ ; (c, f) 20.0  $\mu\text{M}$ .

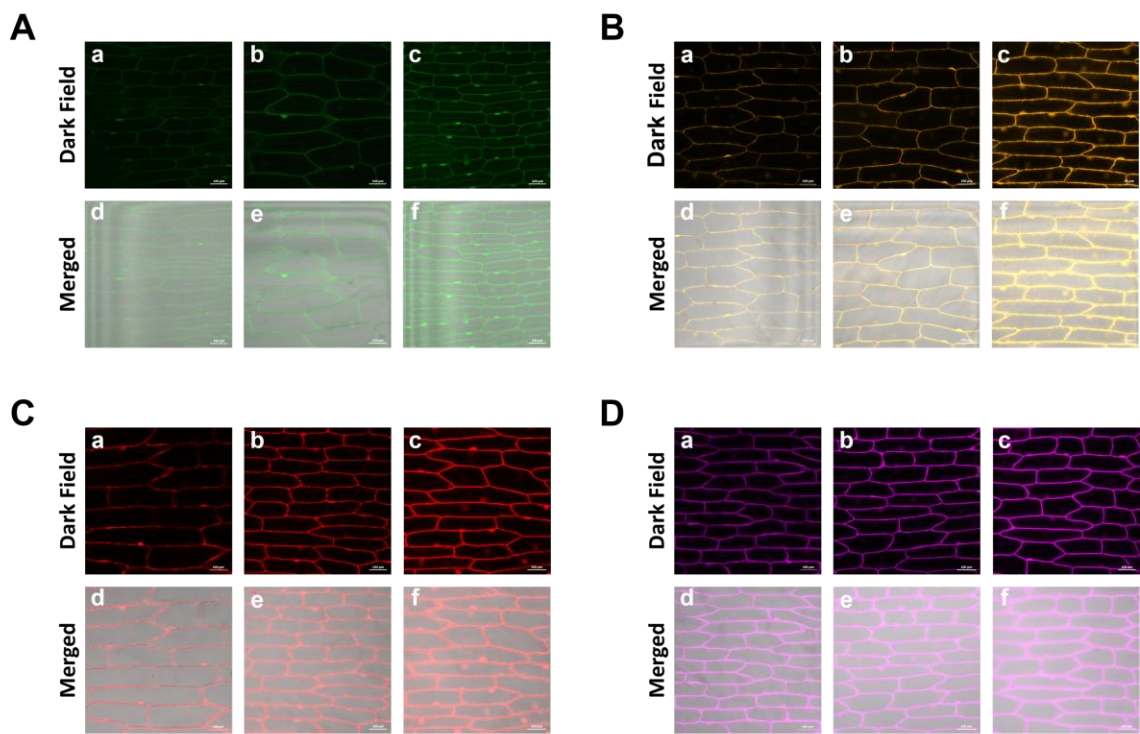


**Figure S7.** Laser scanning confocal microscopy images of onion epidermal cells stained with different amounts of dyes at different staining time. (A) SP-G for 15 min: (a, d) 10.0  $\mu\text{M}$ ; (b, e) 20.0  $\mu\text{M}$ ; (c, f) 30.0  $\mu\text{M}$ ; (B) SQ-O for 15 min: (a, d) 20.0  $\mu\text{M}$ ; (b, e) 30.0  $\mu\text{M}$ ; (c, f) 40.0  $\mu\text{M}$ ; (C) SP-R for 2 min: (a, d) 1.0  $\mu\text{M}$ ; (b, e) 5.0  $\mu\text{M}$ ; (c, f) 10.0  $\mu\text{M}$ ; (D) SQ-NIR for 20 min: (a, d) 10.0  $\mu\text{M}$ ; (b, e) 20.0  $\mu\text{M}$ ; (c, f) 30.0  $\mu\text{M}$ .

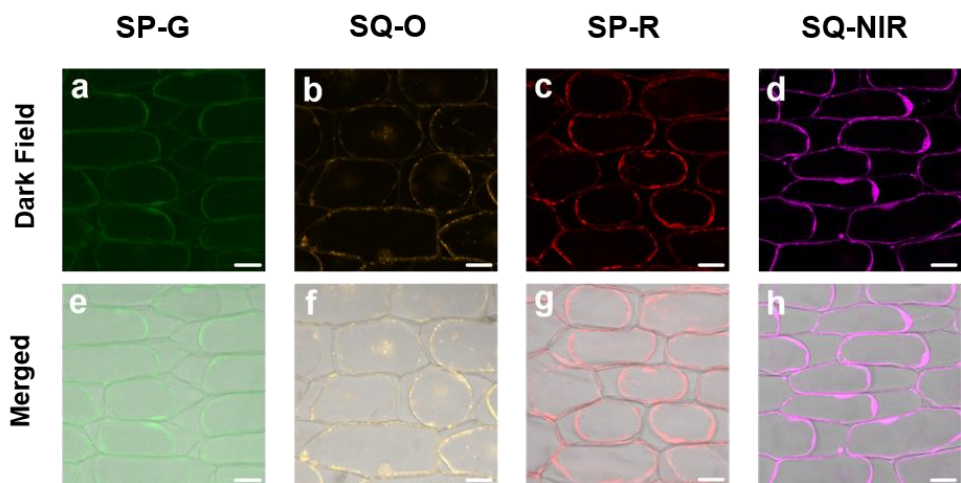


**Figure S8.** Laser scanning confocal microscopy images of onion epidermal cells stained with different control dyes after plasmolysis using a NaCl solution. Plasmolysis was achieved using a NaCl solution of 0.025 g/mL. (a, e) SP-G (50.0  $\mu\text{M}$ , 10 min); (b, f) SQ-O (50.0  $\mu\text{M}$ , 10 min); (c, g) SP-R (10.0  $\mu\text{M}$ , 10 min); (d, h) SQ-NIR (20.0  $\mu\text{M}$ , 10 min). Scale bar = 50  $\mu\text{m}$ .

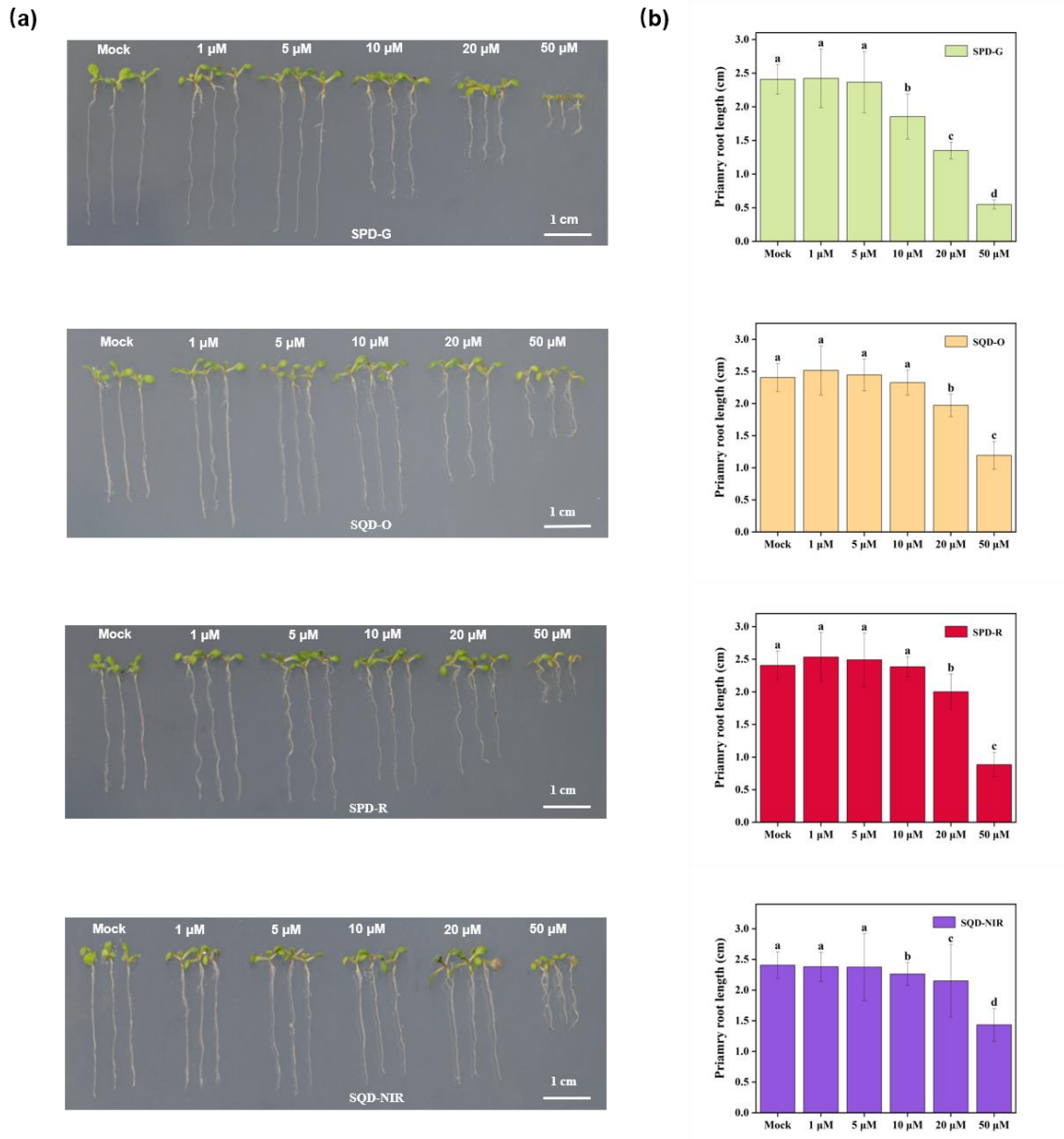


**Figure S9.** (a) Photographs of representative *arabidopsis thaliana* seedlings incubated without (Mock) and with different concentrations of SPD-G, SQD-O, SPD-R, SQD-NIR (1.0  $\mu$ M to 50.0  $\mu$ M) after 6 days. (b) Average root lengths of *arabidopsis thaliana* seedlings incubated without (Mock) and with different concentrations of SPD-G, SQD-O, SPD-R, SQD-NIR (1.0  $\mu$ M to 50.0  $\mu$ M) after 6 days.



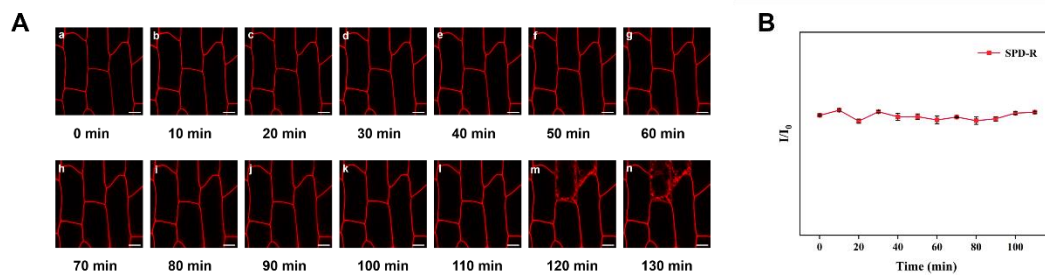


**Figure S10.** The changes of laser scanning confocal microscopy images of onion epidermal cells stained with SPD-R (5.0  $\mu\text{M}$ ) for 2 min versus irradiation time at 561 nm using the excitation source of the used microscope: (a) 0 min; (b) 10 min; (c) 20 min; (d) 30 min; (e) 40 min; (f) 50 min; (g) 60 min; (h) 70 min; (i) 80 min; (j) 90 min; (k) 100 min; (l) 110 min; (m) 120 min; (n) 130 min. Scale bar = 10  $\mu\text{m}$ . (B) The change of PL intensity of SPD-R inside the cell membranes versus irradiation time at 561 nm using the excitation source of the used microscope.

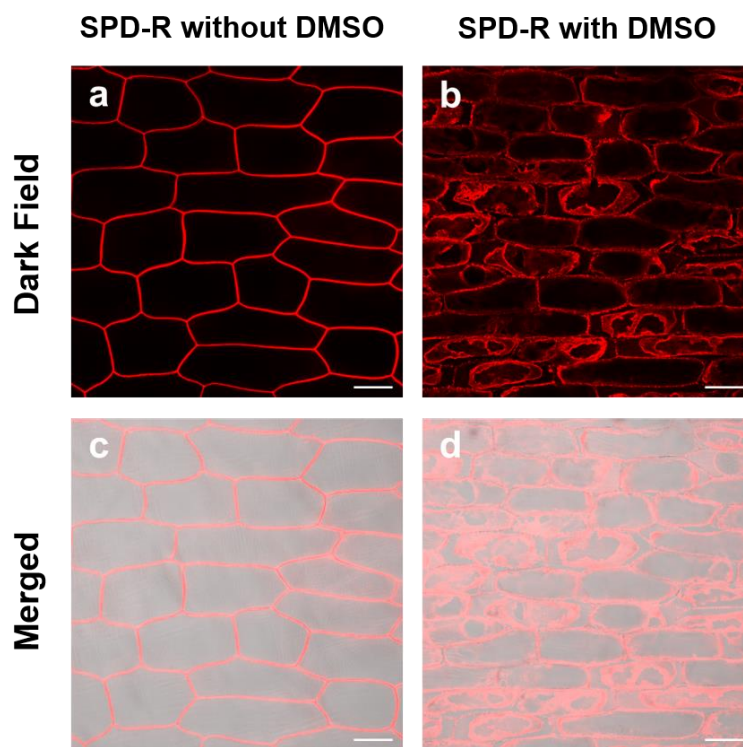


**Figure S11.** Laser scanning confocal microscopy images of onion epidermal cells stained with SPD-R (5.0  $\mu\text{M}$ ) before (a, c) and after treatment of DMSO (b, d). Scale bar = 100  $\mu\text{m}$ .

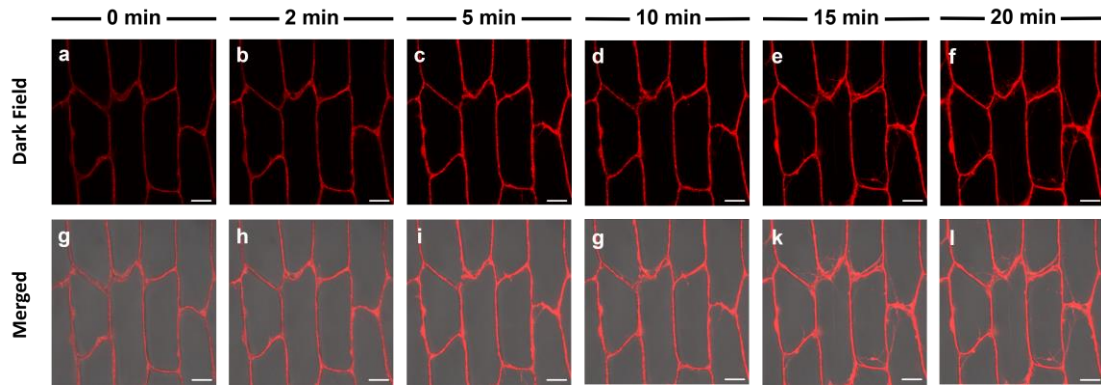


**Figure S12.** Laser scanning confocal microscopy images of onion epidermal cells stained with SP-R (10.0  $\mu$ M) at various time points: (a, g) 0 min; (b, h) 2 min; (c, i) 5 min; (d, j) 10 min; (e, k) 15 min; (f, l) 20 min. Scale bar = 50  $\mu$ m.

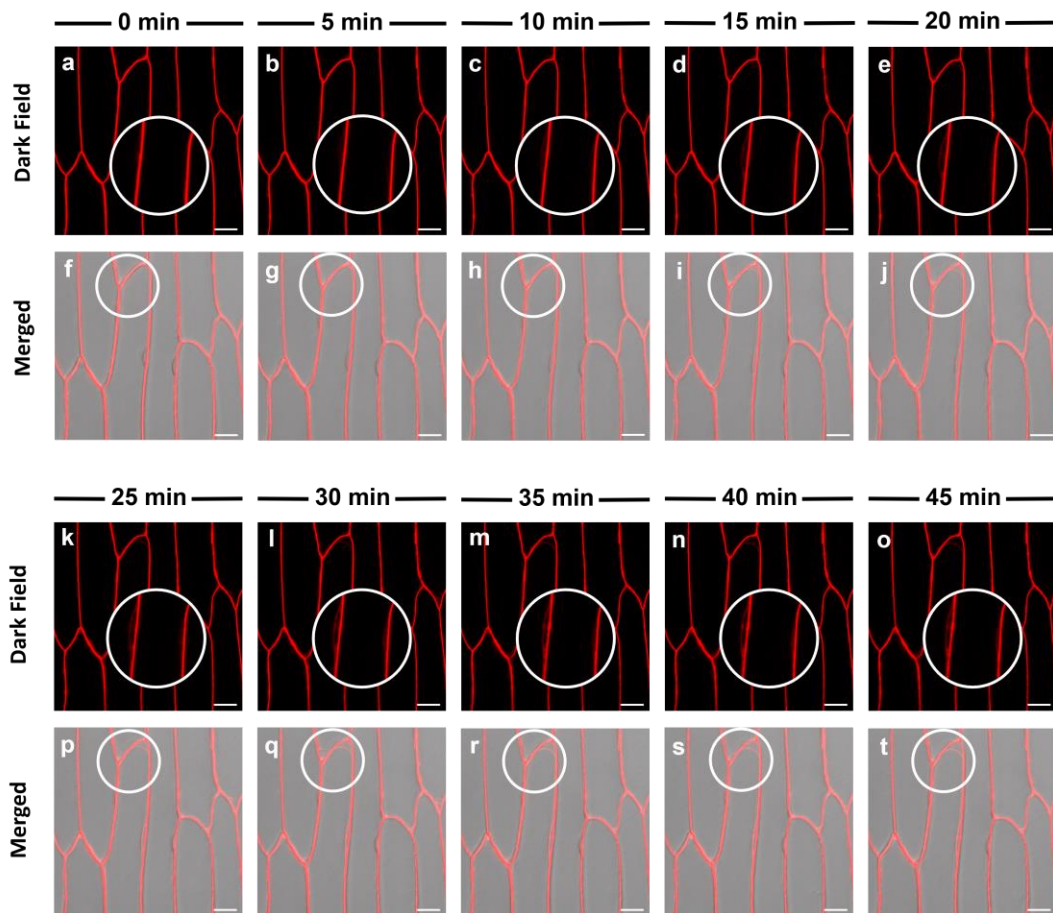


**Figure S13.** Laser scanning confocal microscopy images in onion epidermal cells stained with FM 4-64 (5.0  $\mu$ M) at various time points: (a, f) 0 min; (b, g) 5 min; (c, h) 10 min; (d, i) 15 min; (e, j) 20 min; (p, k) 25 min; (l, q) 30 min; (m, r) 35 min; (n, s) 40 min; (o, t) 45 min. The staining of a portion of nucleus membrane and vacuole membrane were highlighted. Scale bar = 50  $\mu$ m.

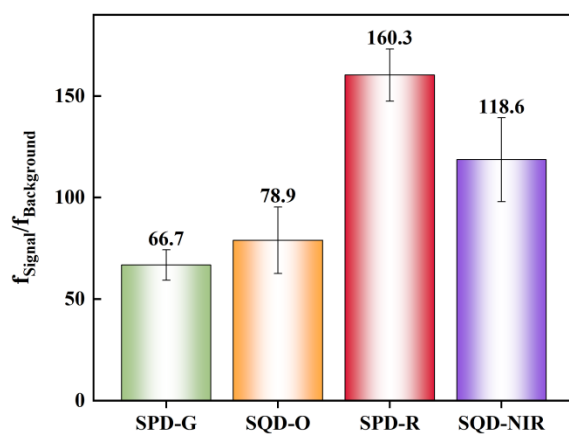


**Figure S14.** The average values of  $f_{\text{Signal}}/f_{\text{Background}}$  for onion epidermal cells stained with different SD dyes in 3D images.

#### 4. Spectra of Compounds

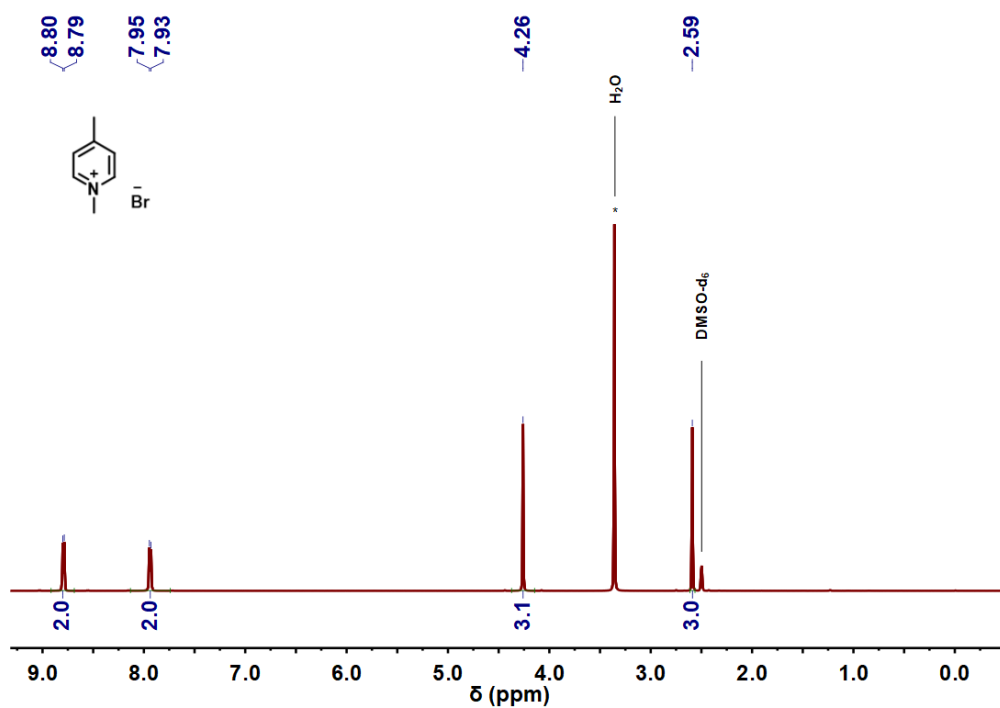


**Figure S15.** <sup>1</sup>H NMR spectra of 1,4-Dimethylpyridinium bromide in DMSO

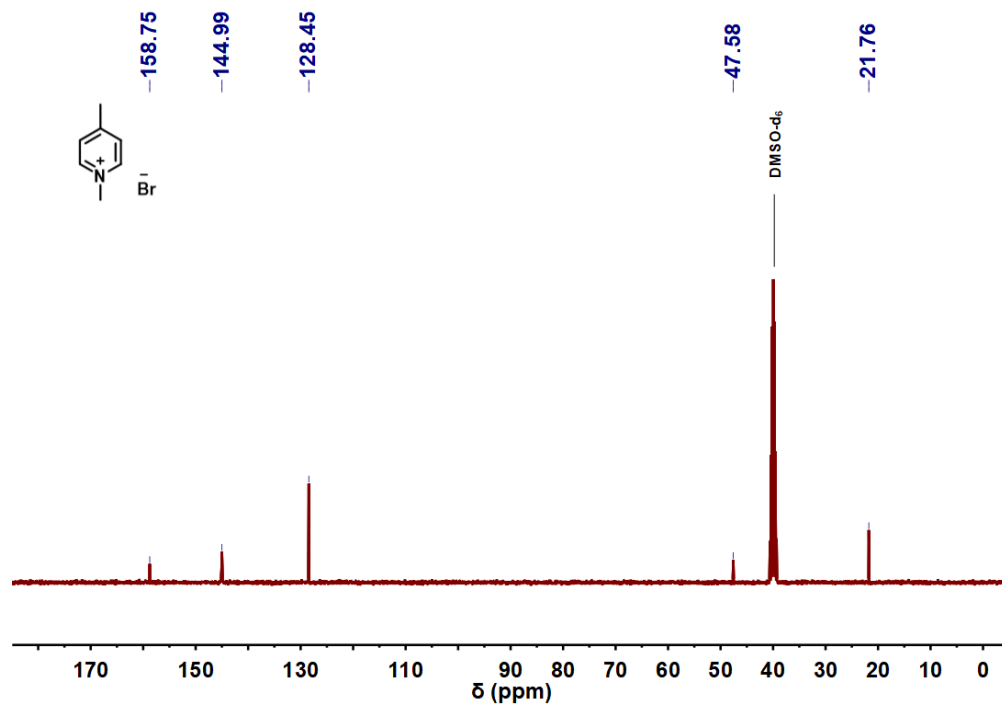


Figure S16. <sup>13</sup>C NMR spectra of 1,4-Dimethylpyridinium bromide in DMSO

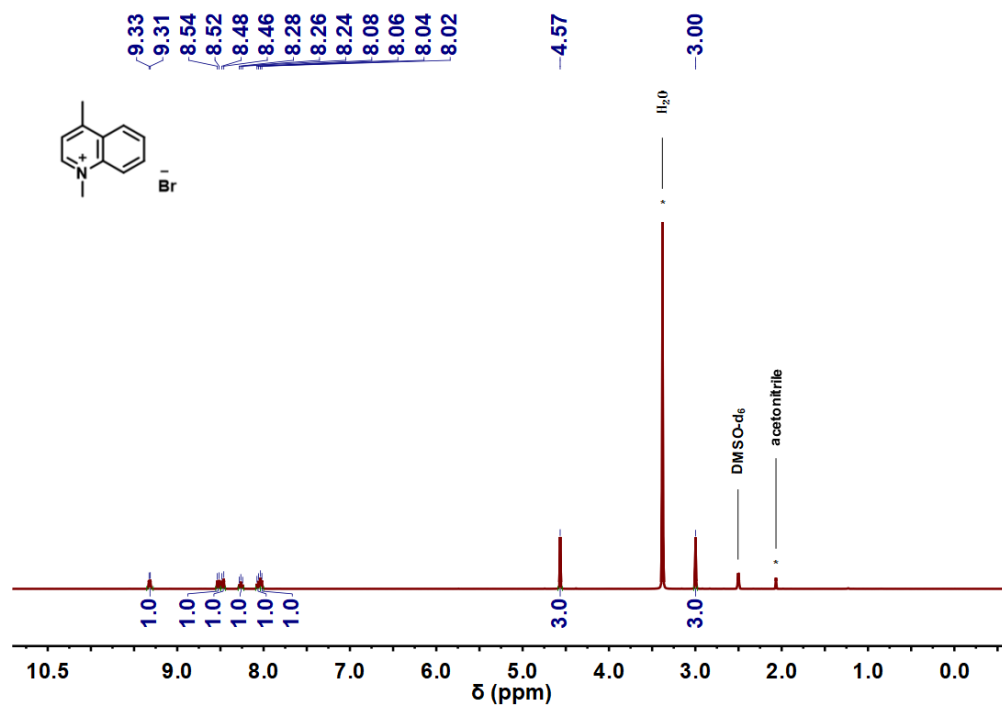


Figure S17. <sup>1</sup>H NMR spectra of 1,4-Dimethylquinolinium bromide in DMSO

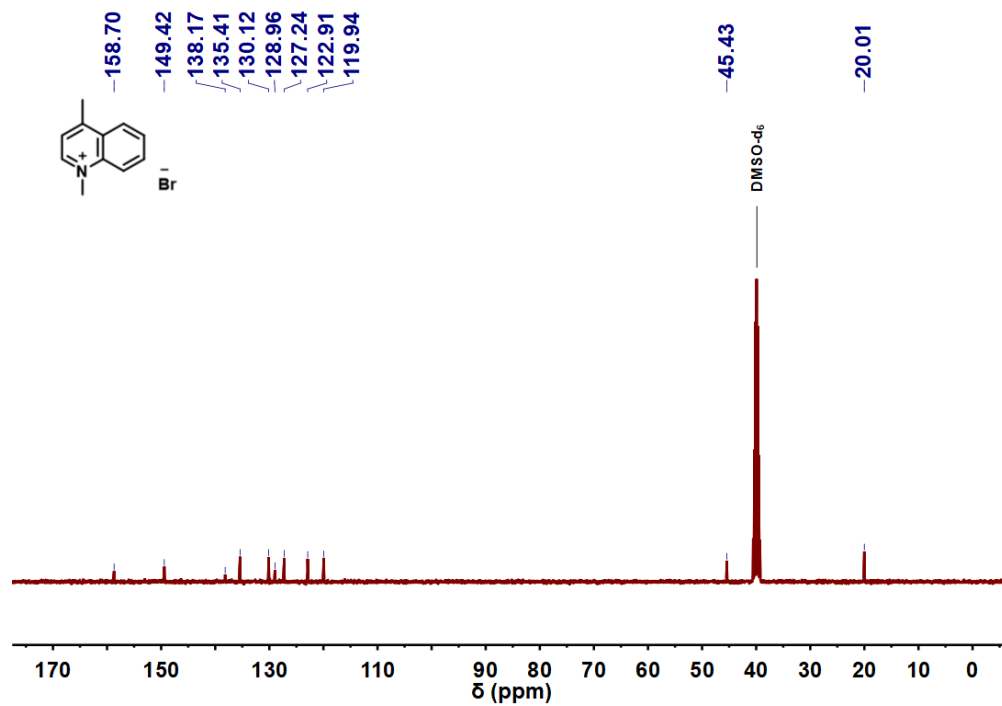


Figure S18.  $^{13}\text{C}$  NMR spectra of 1,4-Dimethylpyridinium bromide in DMSO

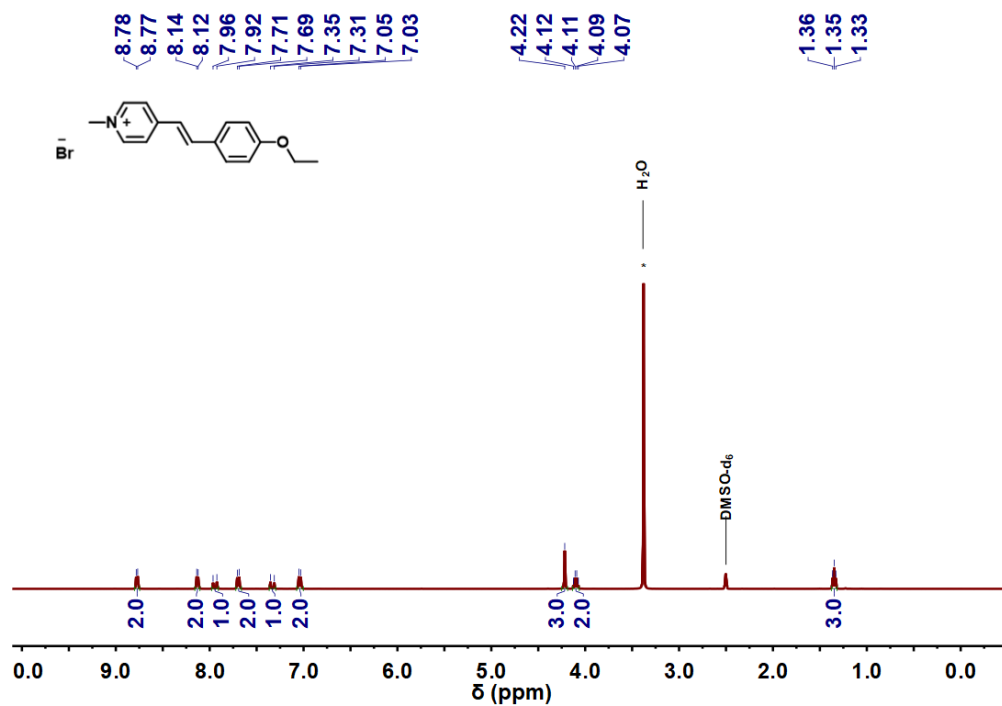


Figure S19.  $^1\text{H}$  NMR spectra of 4-(4-ethoxystyryl)-1-methyl-pyridinium bromide (SP-G) in DMSO

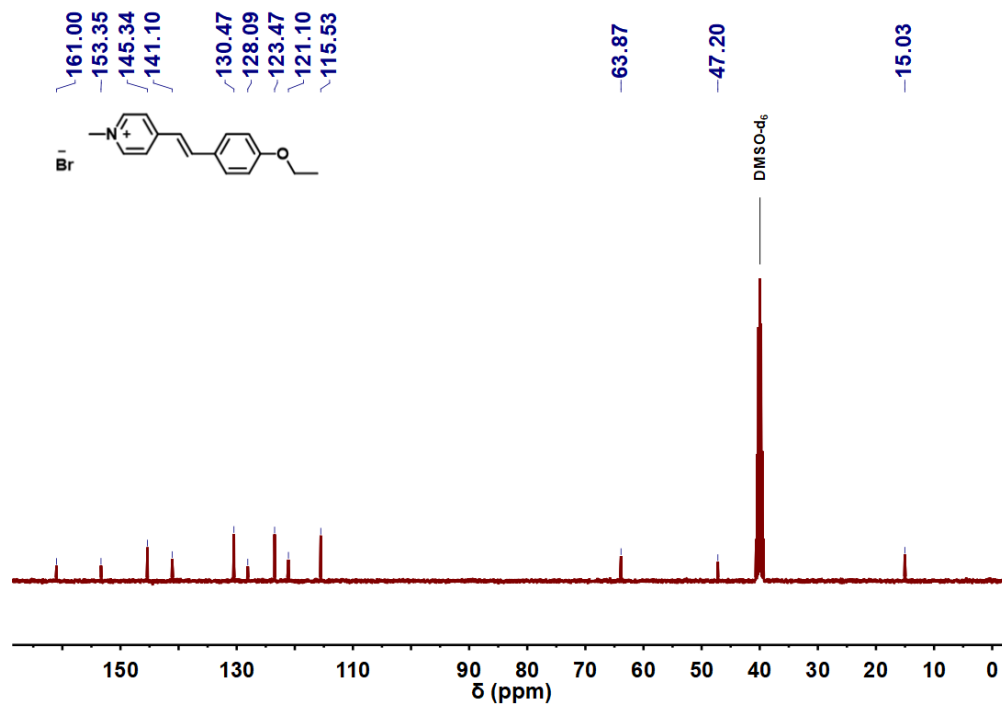


Figure S20.  $^{13}\text{C}$  NMR spectra of 4-(4-ethoxystyryl)-1-methyl-pyridinium bromide (SP-G) in DMSO

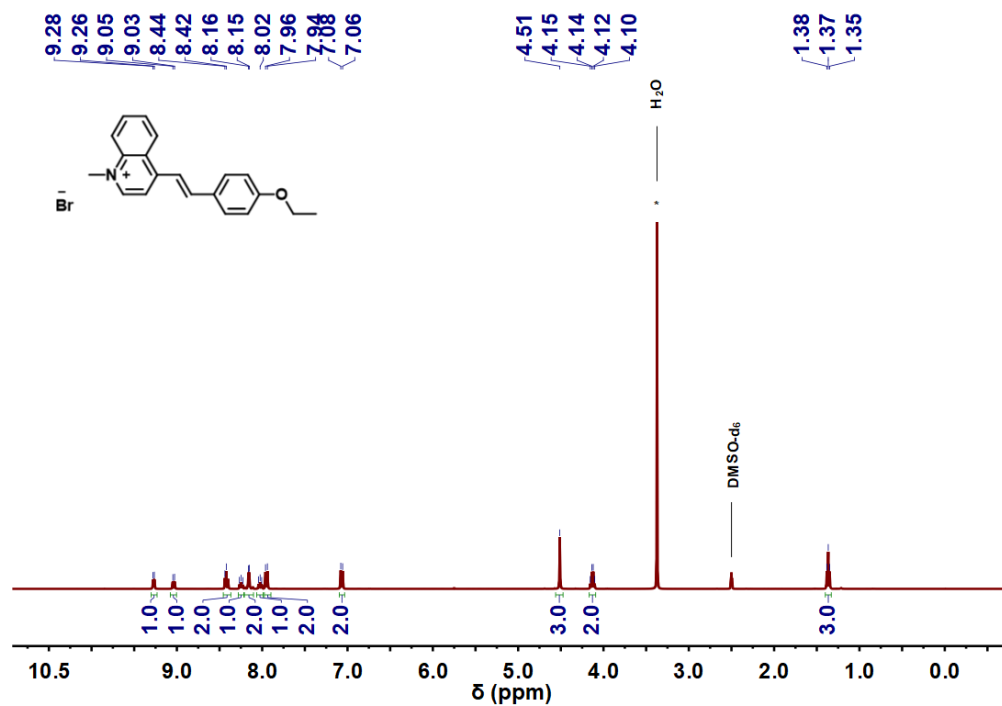


Figure S21.  $^1\text{H}$  NMR spectra of 4-(4-ethoxystyryl)-1-methyl-quinolinium bromide (SQ-O) in DMSO

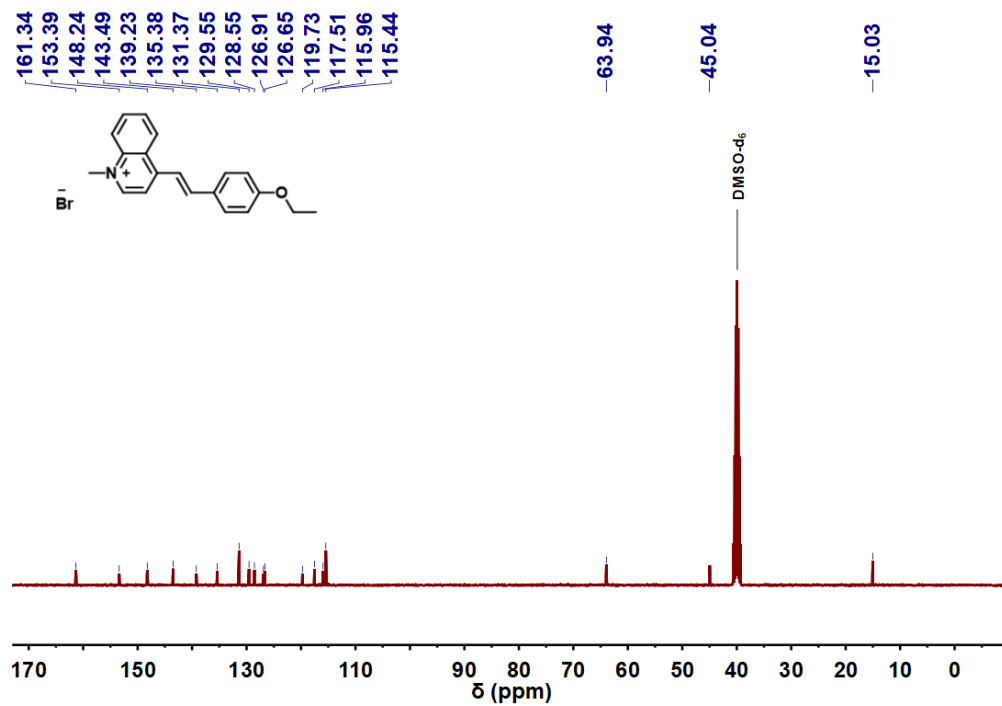


Figure S22.  $^{13}\text{C}$  NMR spectra of 4-(4-ethoxystyryl)-1-methyl-quinolinium bromide (SQ-O) in DMSO

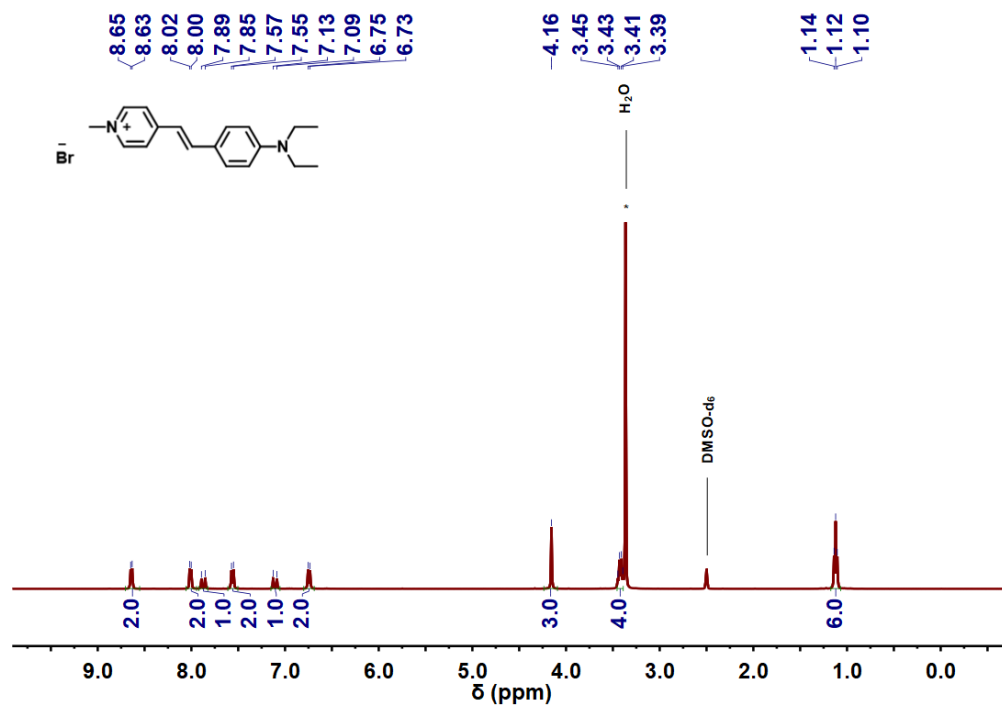
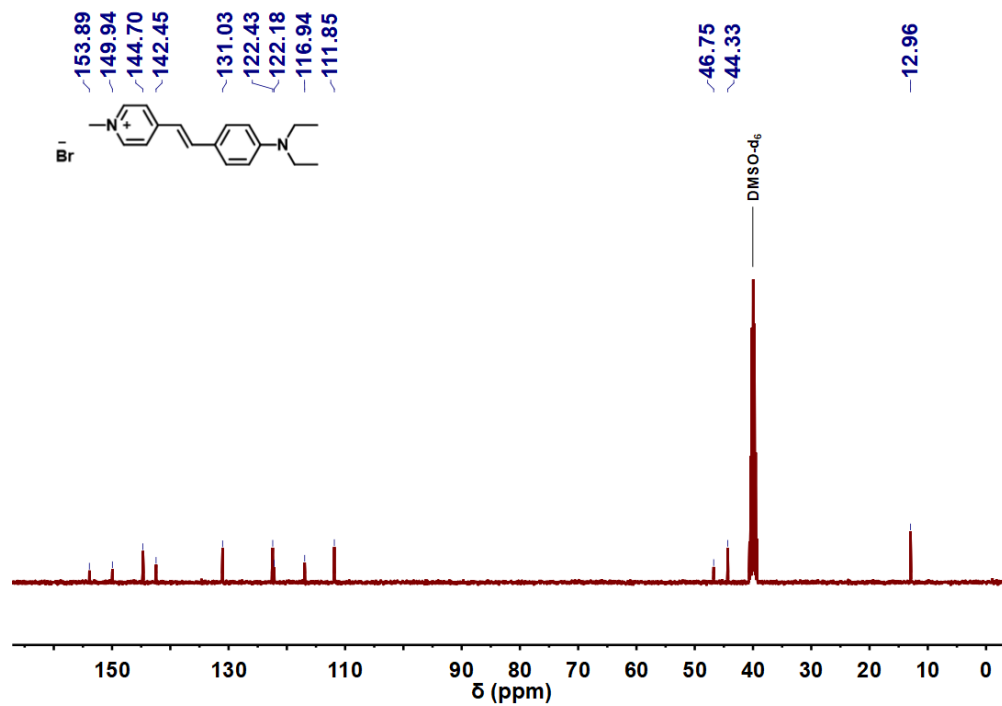
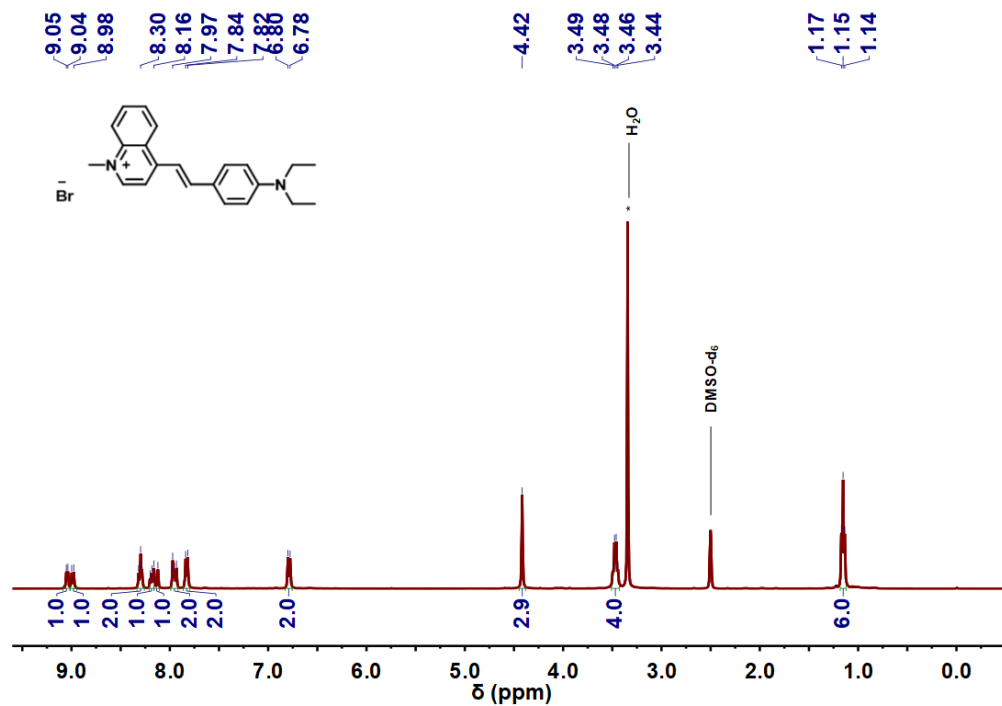


Figure S23.  $^1\text{H}$  NMR spectra of 4-[4-(N,N-diethylamino)styryl]-1-methyl-pyridinium bromide (SP-R) in DMSO



**Figure S24.**  $^{13}\text{C}$  NMR spectra of 4-[4-(N,N-diethylamino)styryl]-1-methyl-pyridinium bromide (SP-R) in DMSO



**Figure S25.**  $^1\text{H}$  NMR spectra of 4-[4-(N,N-diethylamino)styryl]-1-methyl-quinolinium bromide (SQ-NIR) in DMSO



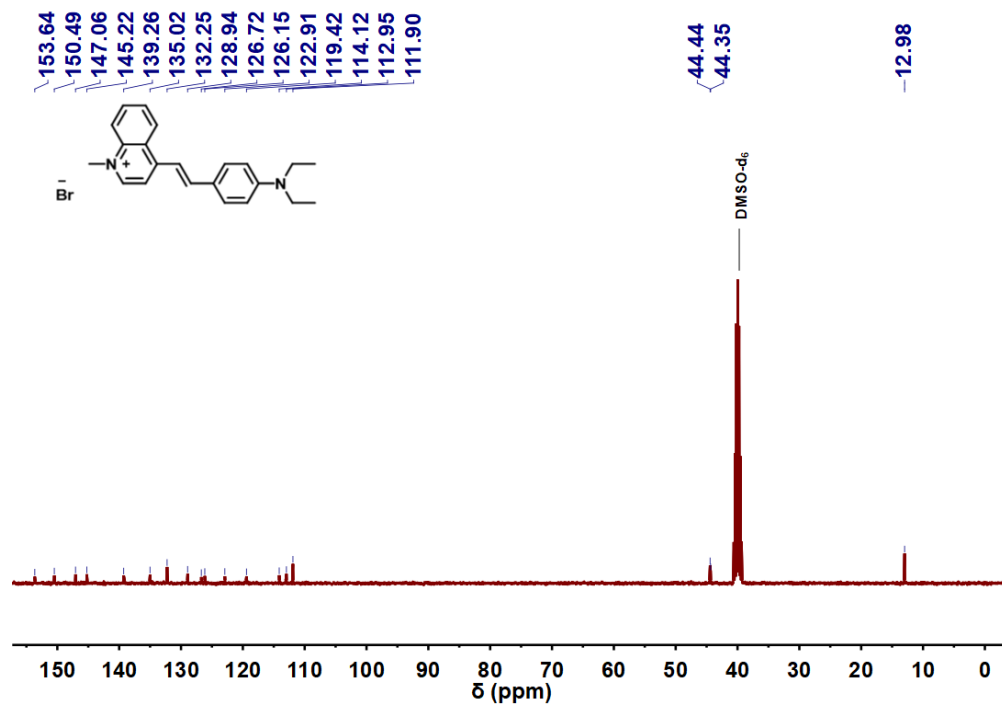


Figure S26.  $^{13}\text{C}$  NMR spectra of 4-[4-(N,N-diethylamino)styryl]-1-methyl-quinolinium bromide (SQ-NIR) in DMSO

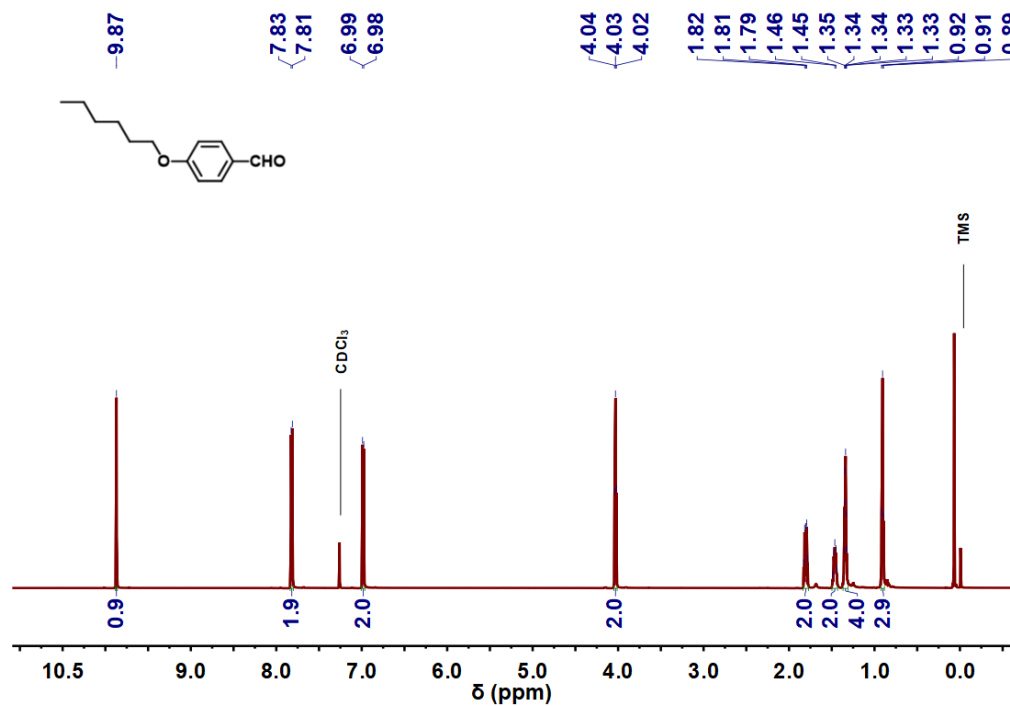


Figure S27.  $^1\text{H}$  NMR spectra of 4-(hexyloxy)benzaldehyde in  $\text{CDCl}_3$

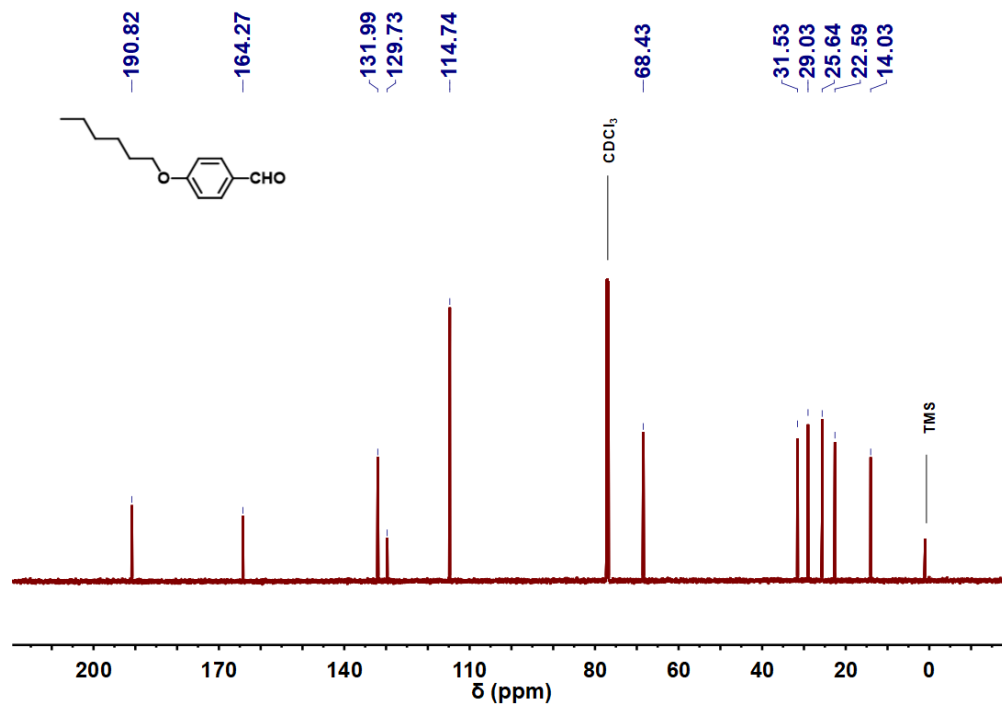


Figure S28.  $^{13}\text{C}$  NMR spectra of 4-(hexyloxy)benzaldehyde in  $\text{CDCl}_3$

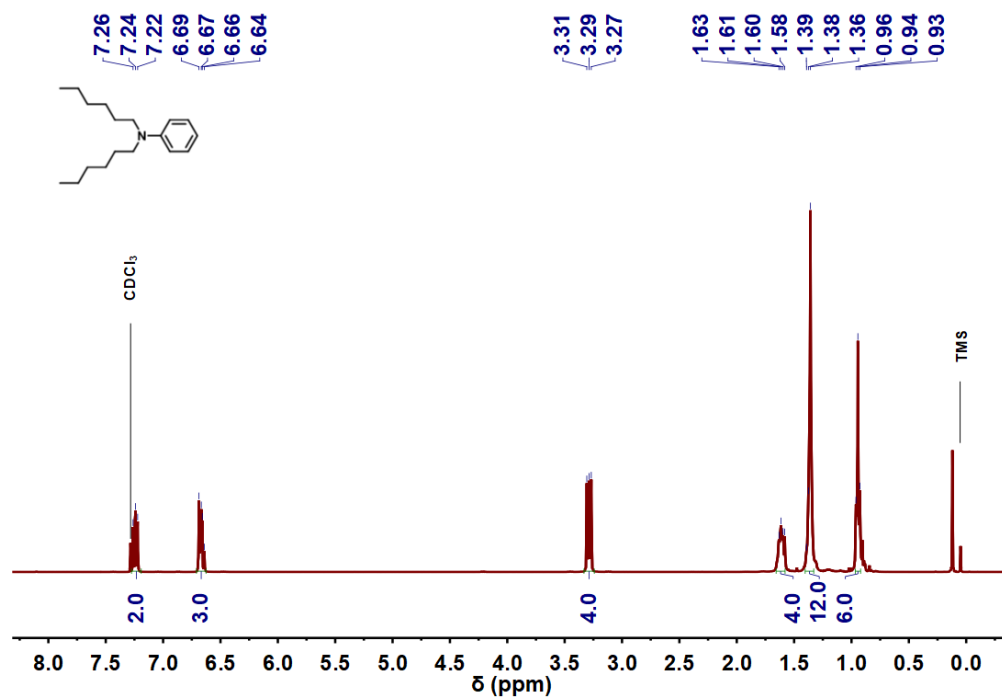


Figure S29.  $^1\text{H}$  NMR spectra of N,N-dihexylaniline in  $\text{CDCl}_3$

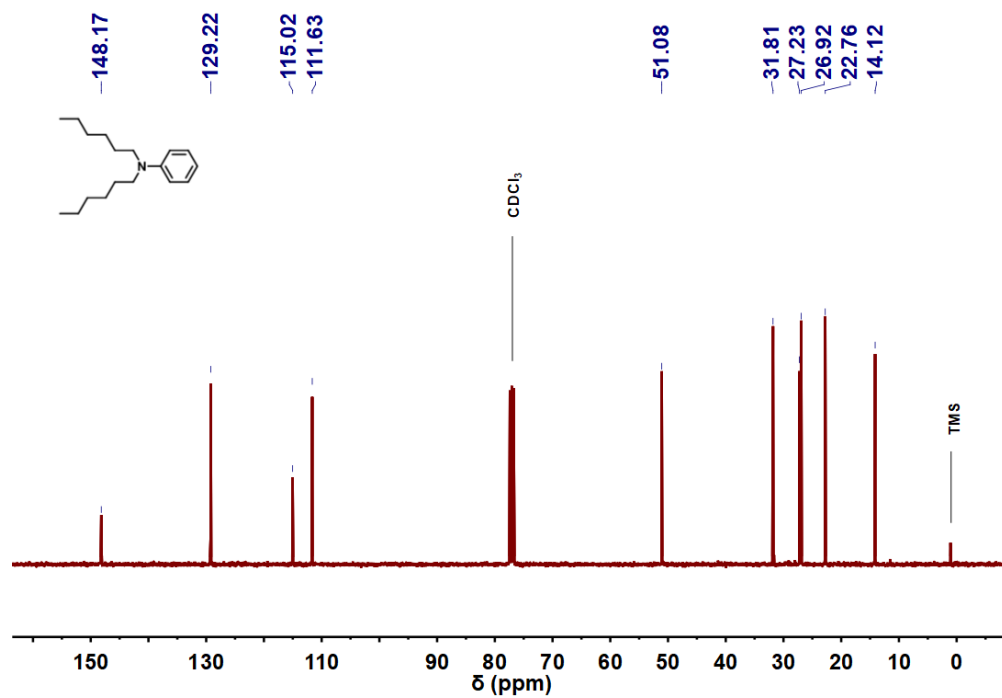


Figure S30.  $^{13}\text{C}$  NMR spectra of N,N-dihexylaniline in CDCl<sub>3</sub>

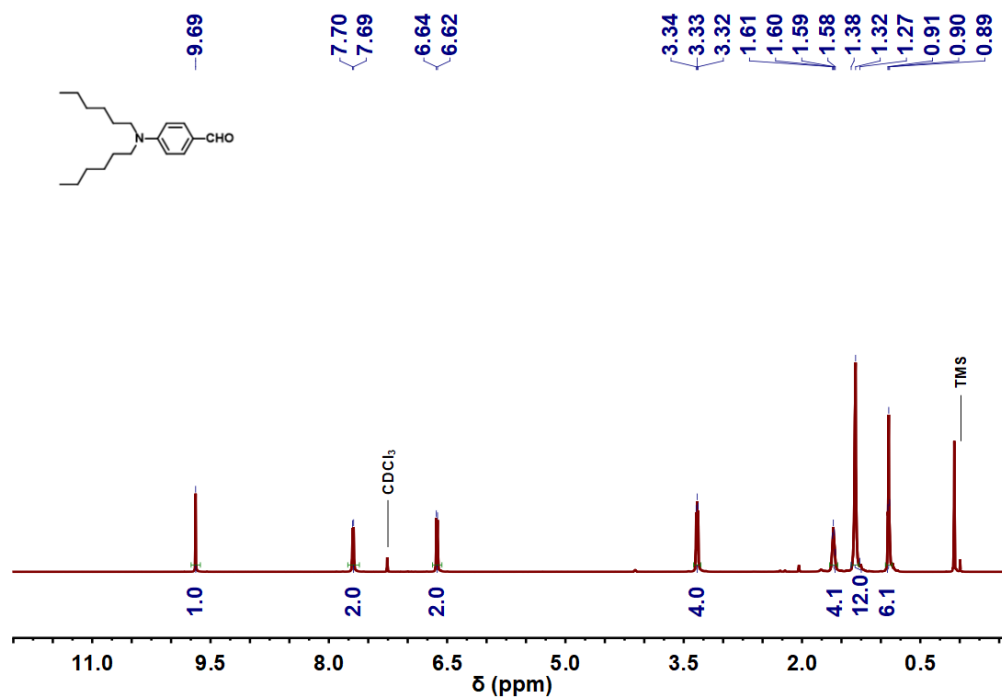


Figure S31.  $^1\text{H}$  NMR spectra of 4-(dihexylamino)benzaldehyde in CDCl<sub>3</sub>

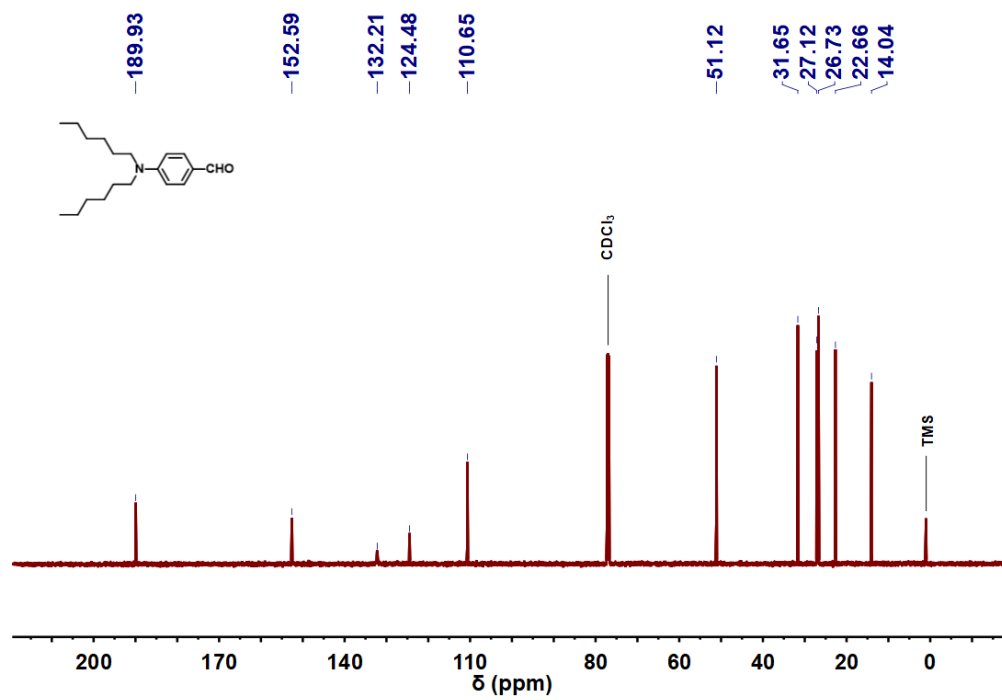


Figure S32.  $^{13}\text{C}$  NMR spectra of 4-(dihexylamino)benzaldehyde in  $\text{CDCl}_3$

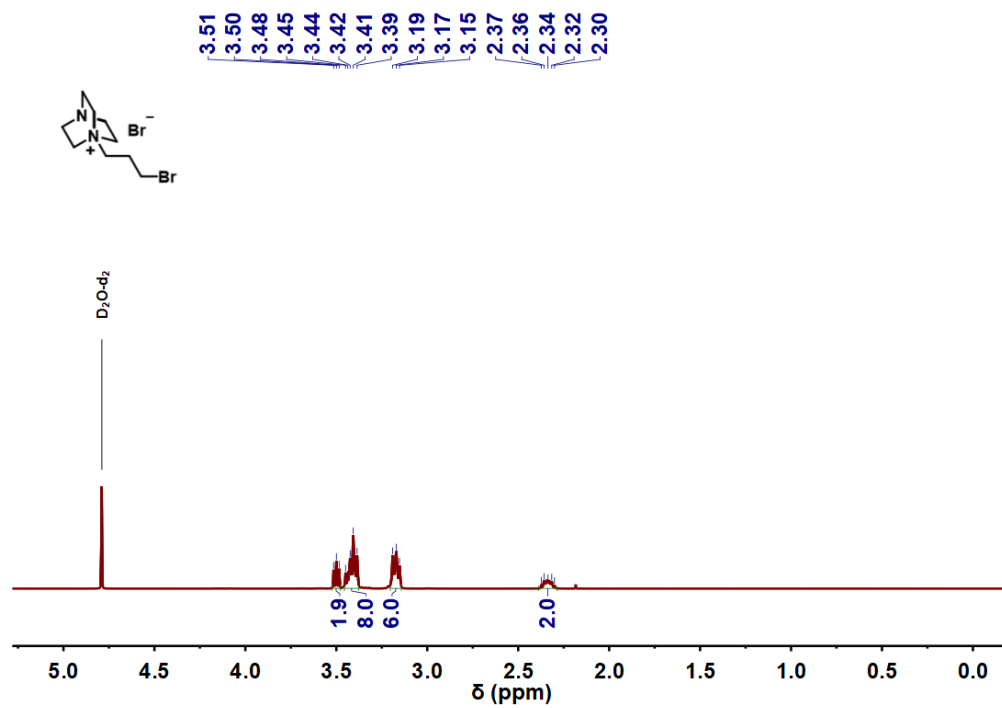


Figure S33.  $^1\text{H}$  NMR spectra of 1-(3-bromopropyl)-1,4-diazabicyclo[2.2.2]octan-1-ium bromide in  $\text{D}_2\text{O}$

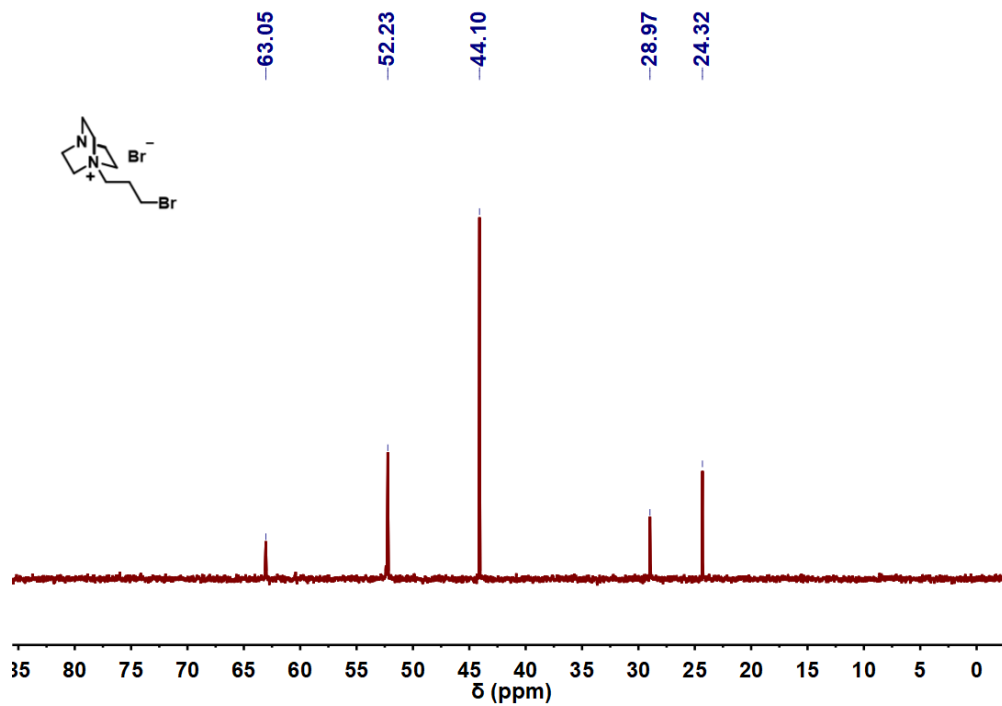


Figure S34.  $^{13}\text{C}$  NMR spectra of 1-(3-bromopropyl)-1,4-diazabicyclo[2.2.2]octan-1-ium bromide in  $\text{D}_2\text{O}$

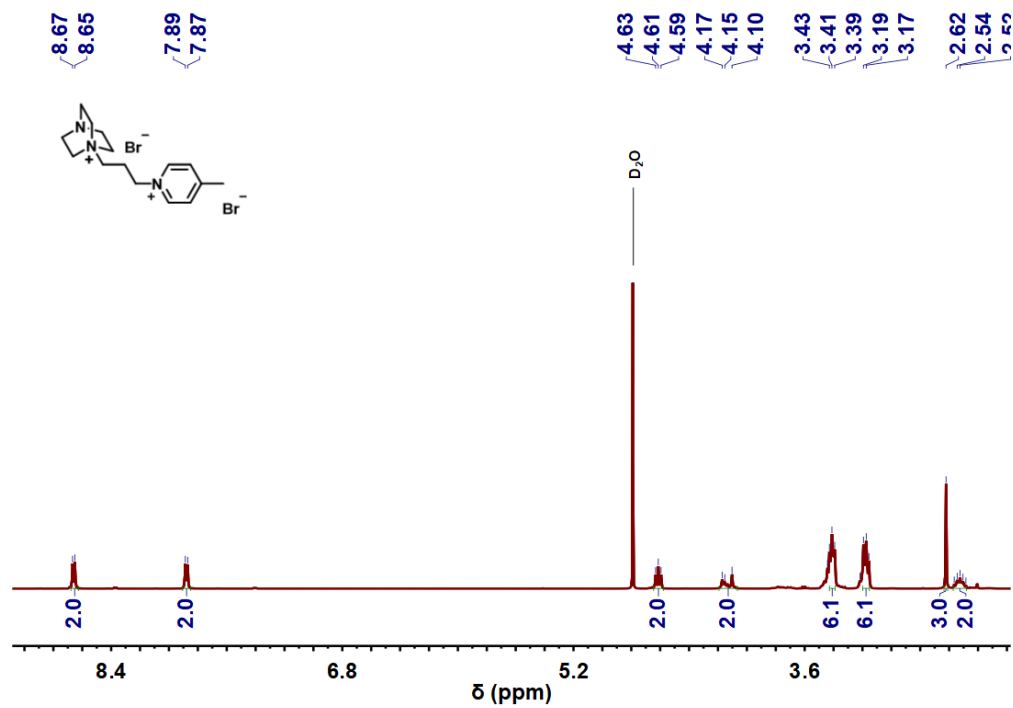


Figure S35.  $^1\text{H}$  NMR spectra of 1-(3-(4-methylpyridin-1-ium-1-yl)propyl)-1,4-diazabicyclo[2.2.2]octan-1-ium dibromide in  $\text{D}_2\text{O}$

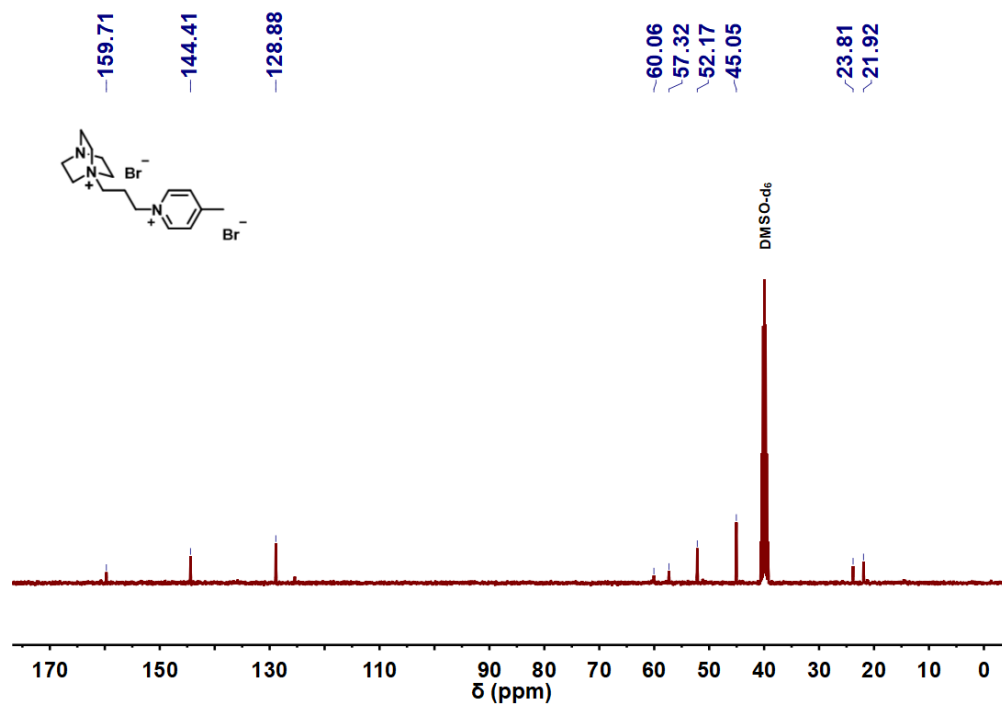


Figure S36.  $^{13}\text{C}$  NMR spectra of 1-(3-(4-methylpyridin-1-ium-1-yl)propyl)-1,4-diazabicyclo[2.2.2]octan-1-ium dibromide in DMSO

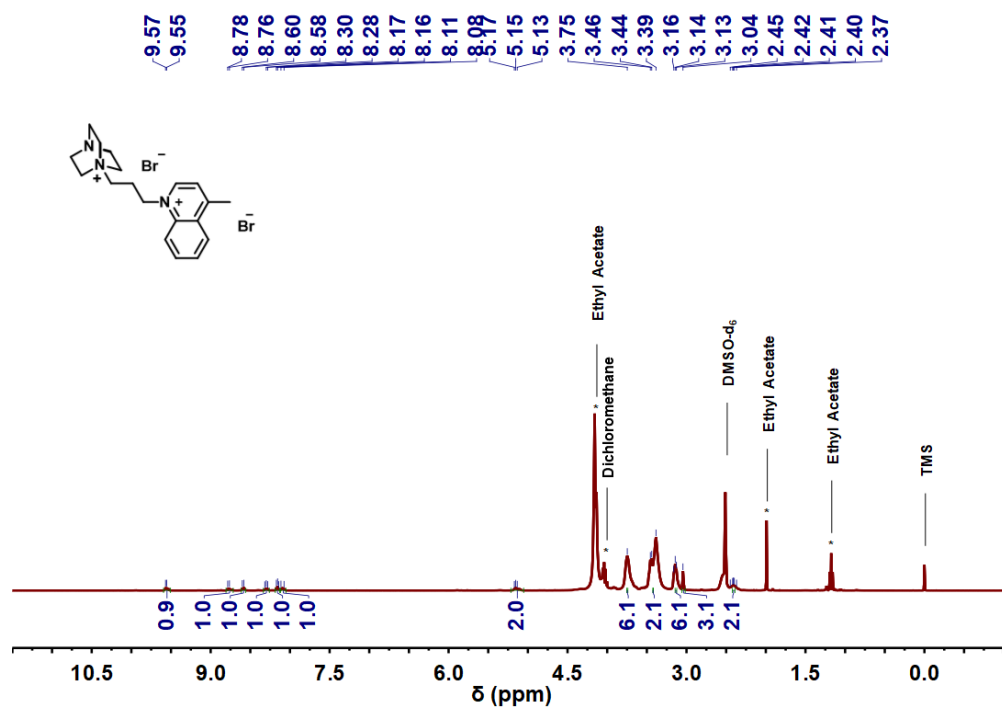
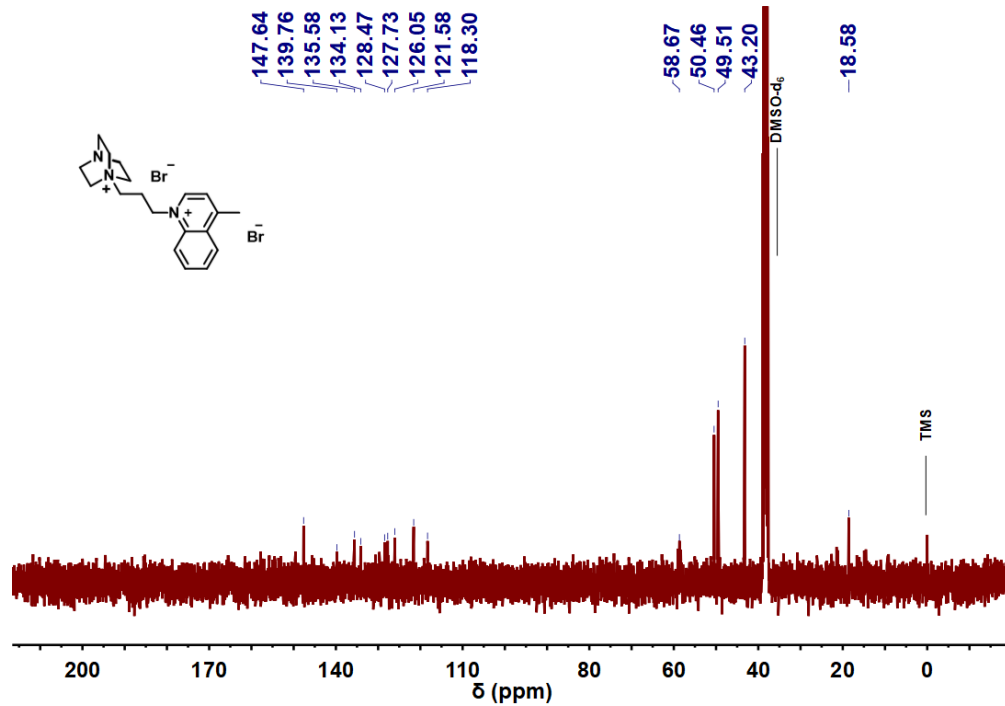
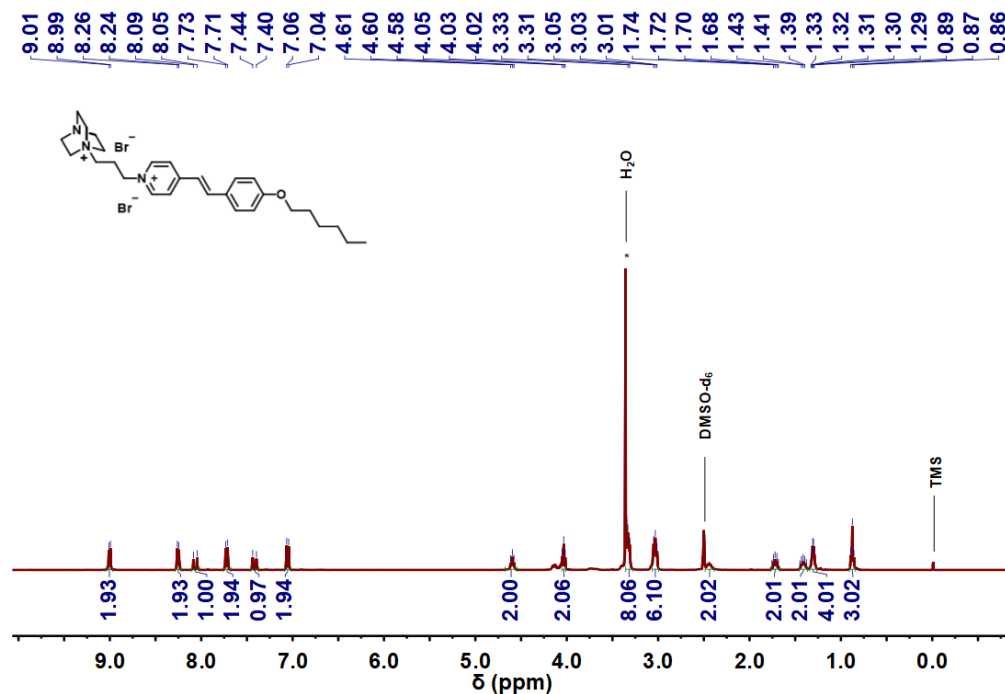


Figure S37.  $^1\text{H}$  NMR spectra of 1-(3-(4-methylquinolin-1-ium-1-yl)propyl)-1,4-diazabicyclo[2.2.2]octan-1-ium dibromide in DMSO



**Figure S38.**  $^{13}\text{C}$  NMR spectra of 1-(3-(4-methylquinolin-1-ium-1-yl)propyl)-1,4-diazabicyclo[2.2.2]octan-1-ium dibromide in DMSO



**Figure S39.**  $^1\text{H}$  NMR spectra of 1-(3-(4-(4-(hexyloxy)styryl)pyridin-1-ium-1-yl)propyl)-1,4-diazabicyclo[2.2.2]octan-1-ium dibromide (SPD-G) in DMSO

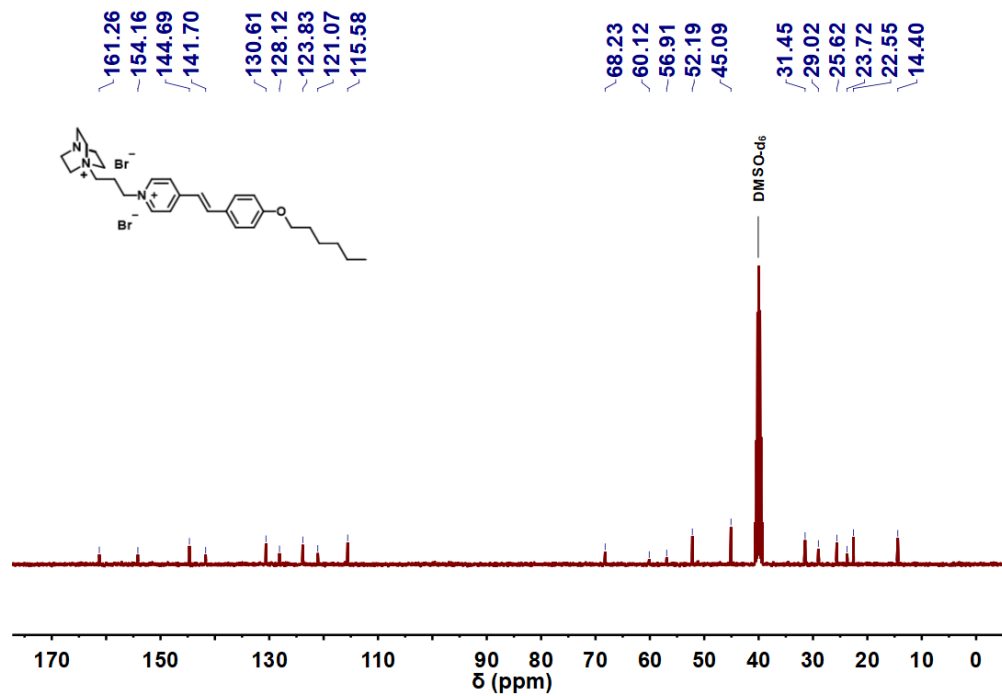


**Figure S40.** <sup>13</sup>C NMR spectra of 1-(3-(4-(4-(hexyloxy)styryl)pyridin-1-ium-1-yl)propyl)-1,4-diazabicyclo[2.2.2]octan-1-ium dibromide (SPD-G) in DMSO

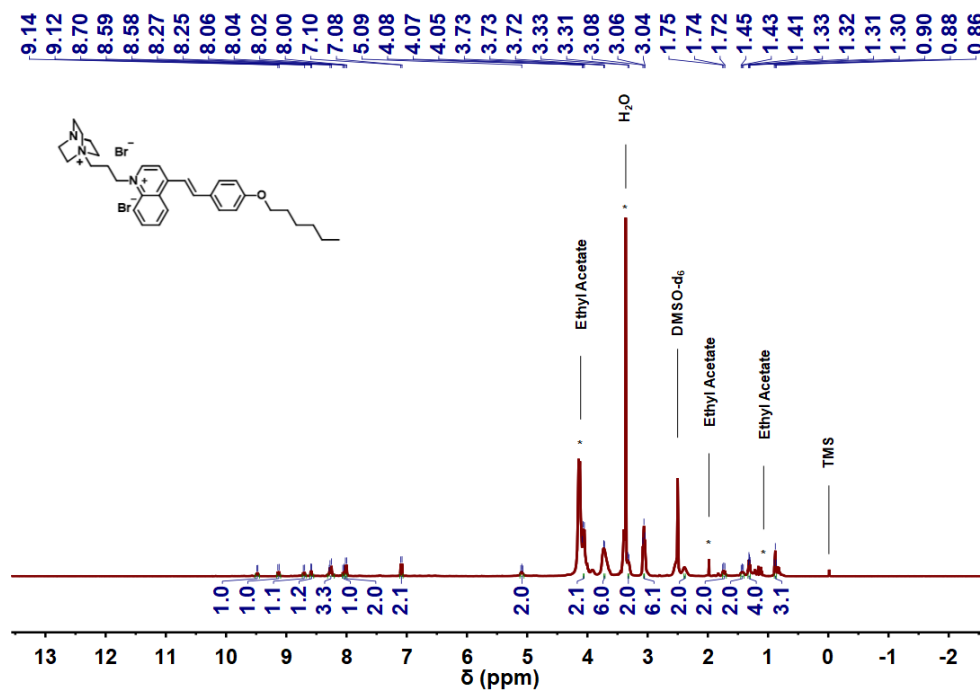


**Figure S41.** <sup>1</sup>H NMR spectra of 1-(3-(4-(4-(dihexylamino)styryl)quinolin-1-ium-1-yl)propyl)-1,4-diazabicyclo[2.2.2]octan-1-ium dibromide (SQD-O) in DMSO



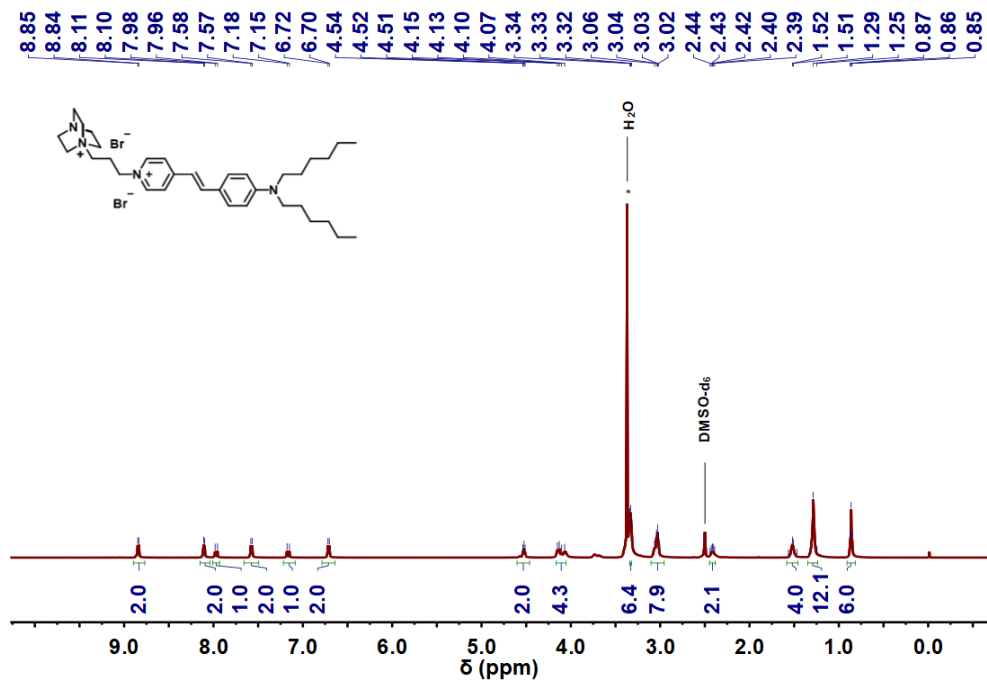


**Figure S42.**  $^1\text{H}$  NMR spectra of 1-(3-(4-(4-(hexyloxy)styryl)pyridin-1-ium-1-yl)propyl)-1,4-diazabicyclo[2.2.2]octan-1-ium dibromide (SPD-R) in DMSO

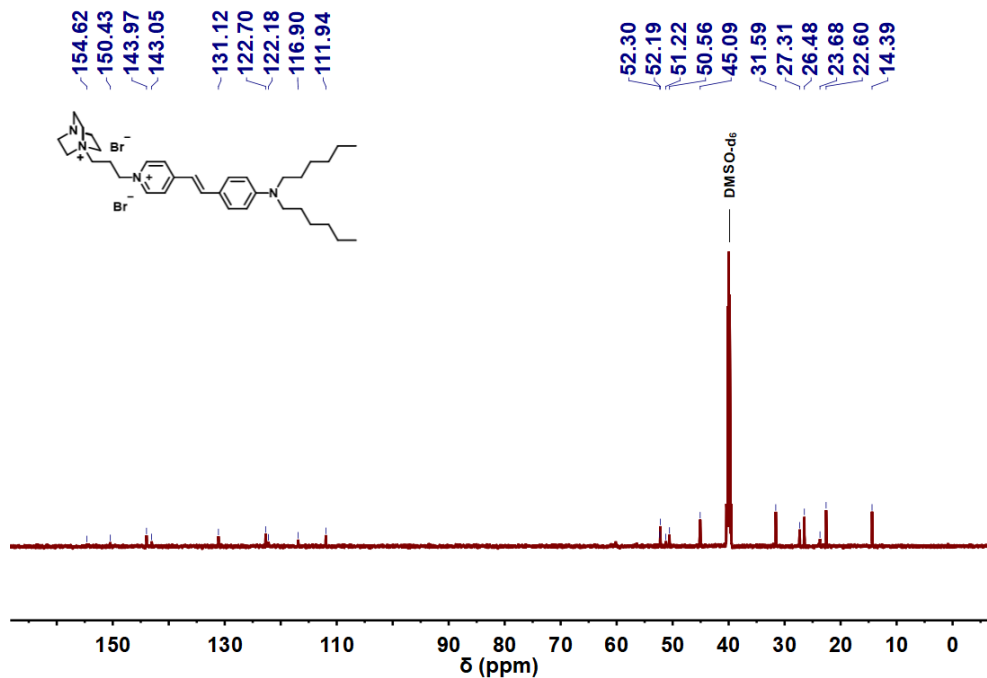


**Figure S43.**  $^{13}\text{C}$  NMR spectra of 1-(3-(4-(4-(hexyloxy)styryl)pyridin-1-ium-1-yl)propyl)-1,4-diazabicyclo[2.2.2]octan-1-ium dibromide (SPD-R) SQD-NIR in DMSO

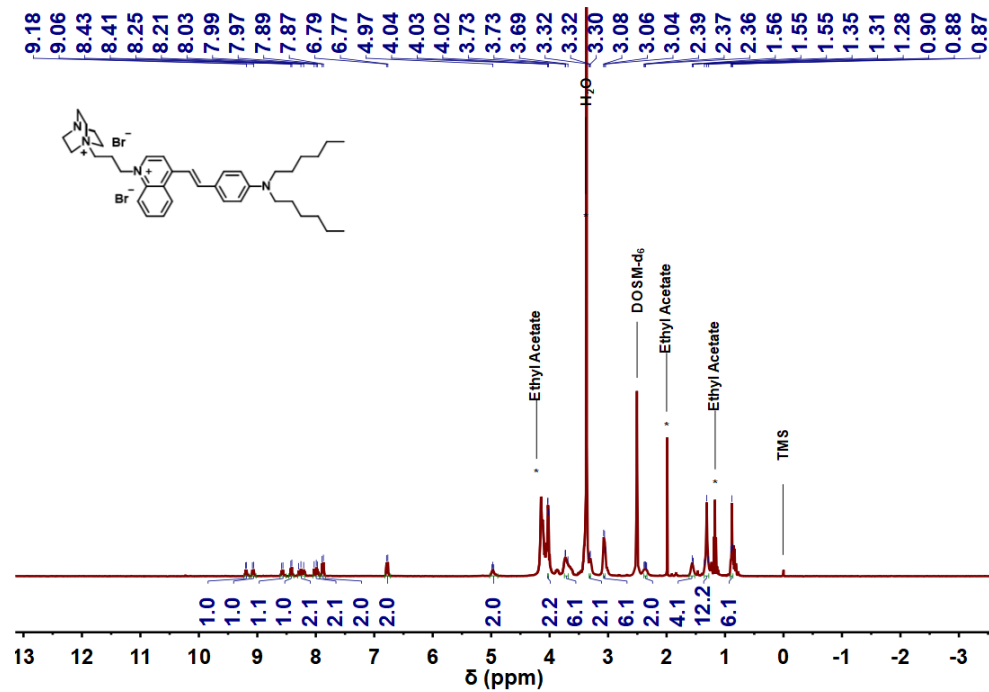


**Figure S44.** <sup>1</sup>H NMR spectra of 1-(3-(4-(4-(dihexylamino)styryl)quinolin-1-ium-1-yl)propyl)-1,4-diazabicyclo[2.2.2]octan-1-ium bromide (SQD-NIR) in DMSO

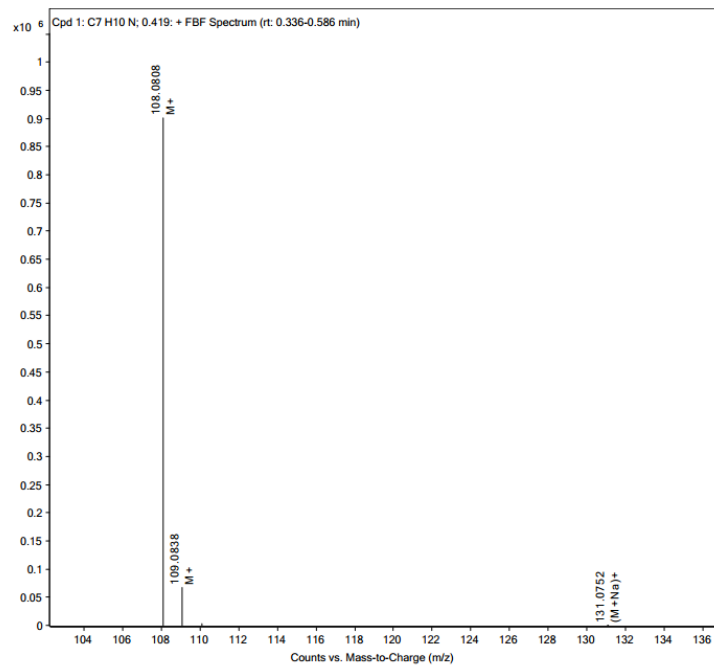


**Figure S45.** High-resolution mass spectrum of 1,4-Dimethylpyridine bromide

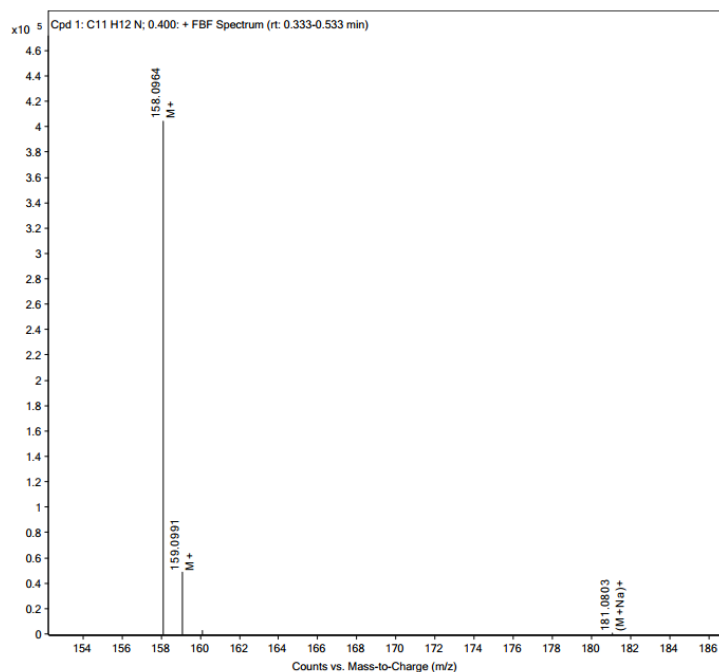


**Figure S46.** High-resolution mass spectrum of 1,4-Dimethylquinolinium bromide

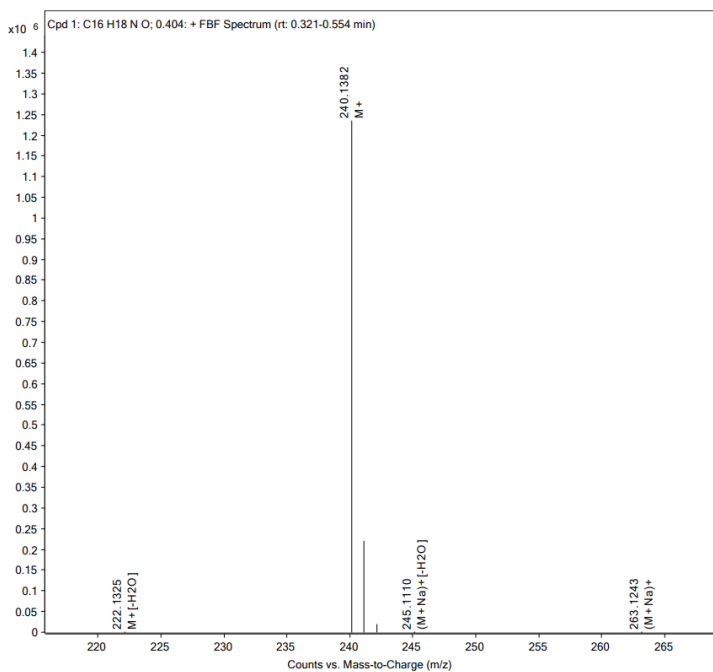


**Figure S47.** High-resolution mass spectrum of 4-(4-ethoxystyryl)-1-methyl-pyridinium bromide (SP-G)

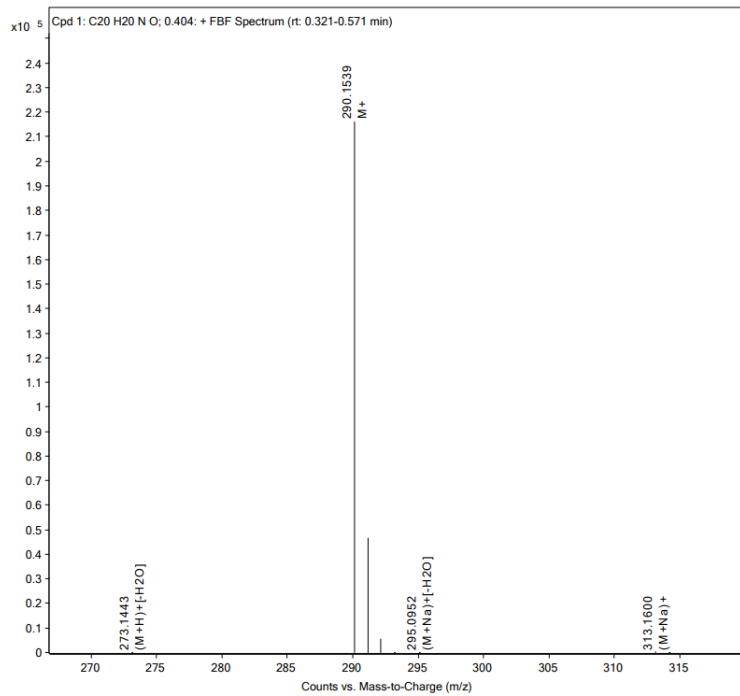


**Figure S48.** High-resolution mass spectrum of 4-(4-ethoxystyryl)-1-methyl-quinolinium bromide (SQ-O)

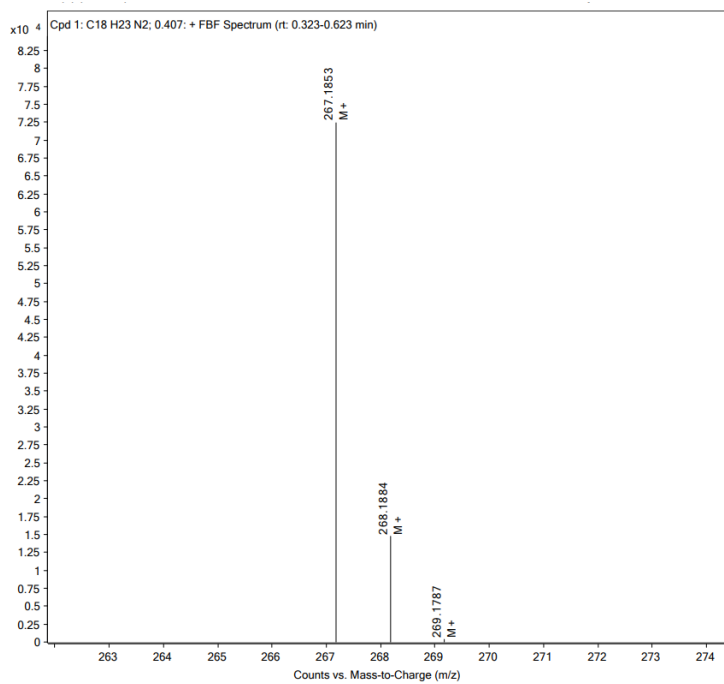


**Figure S49.** High-resolution mass spectrum of 4-[4-(N,N-diethylamino)styryl]-1-methyl-pyridinium bromide (SP-R)

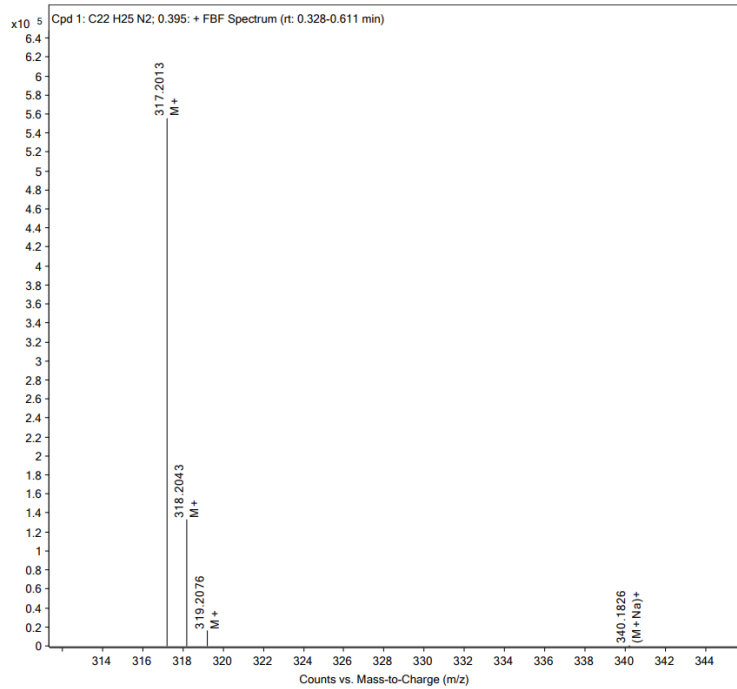


**Figure S50.** High-resolution mass spectrum of 4-[4-(N,N-diethylamino)styryl]-1-methyl-quinolinium bromide (SQ-NIR)

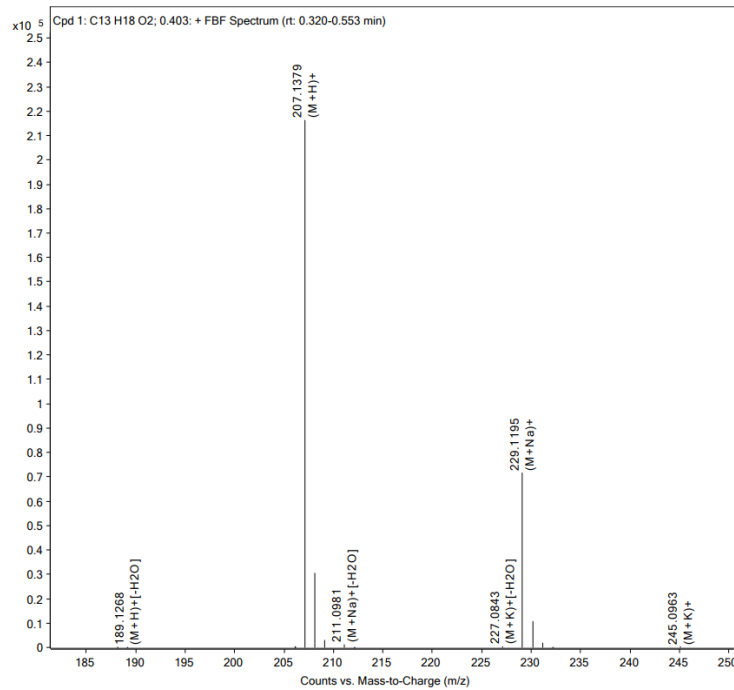


**Figure S51.** High-resolution mass spectrum of 4-(hexyloxy)benzaldehyde

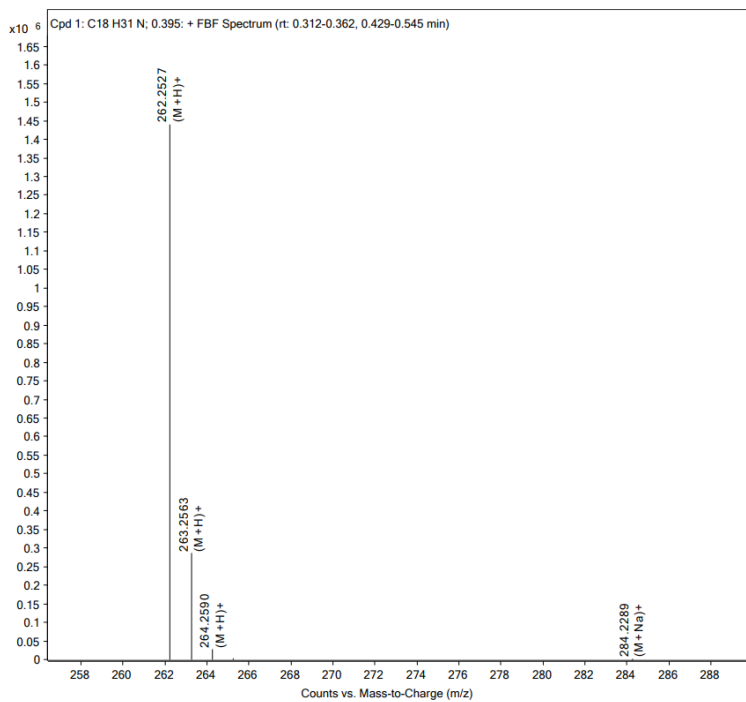


**Figure S52.** High-resolution mass spectrum of N,N-dihexylaniline

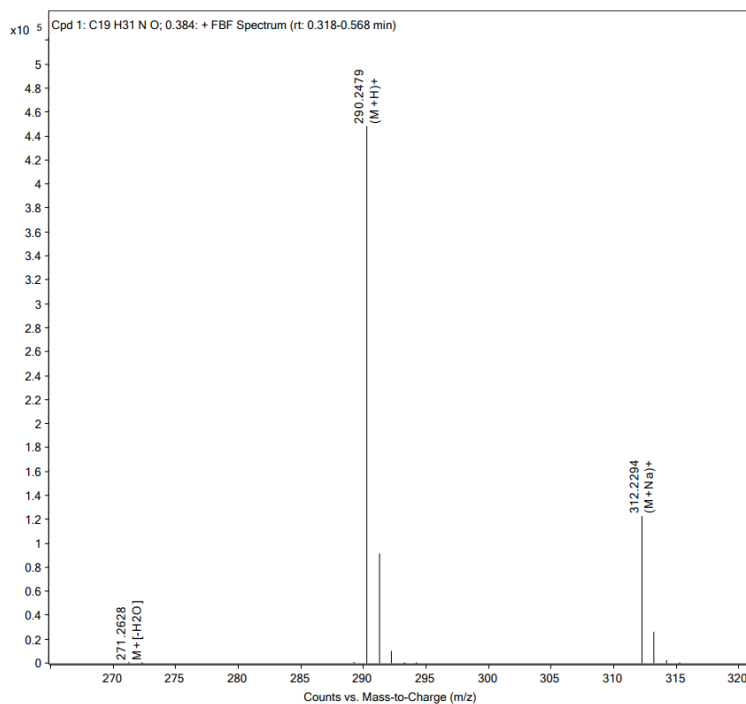


**Figure S53.** High-resolution mass spectrum of 4-(dihexylamino)benzaldehyde

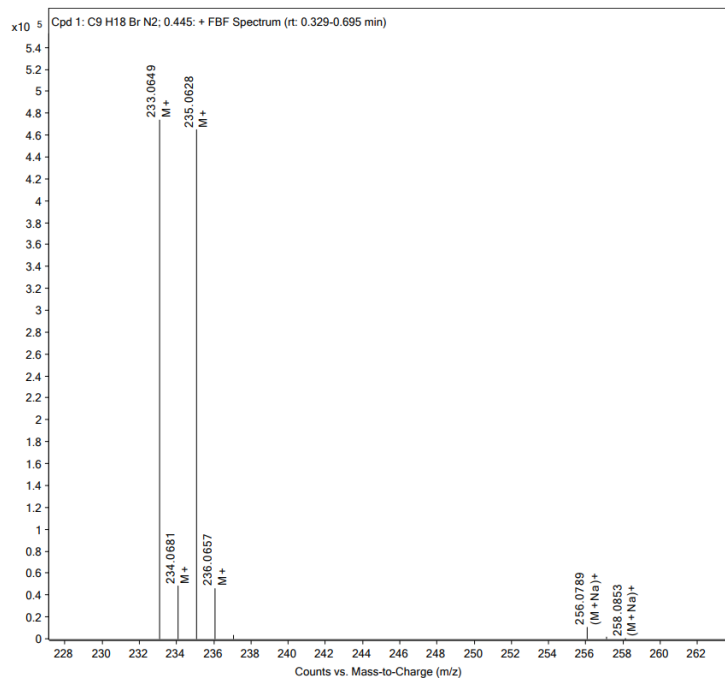


**Figure S54.** High-resolution mass spectrum of 1-(3-bromopropyl)-1,4-diazabicyclo[2.2.2]octan-1-ium bromide

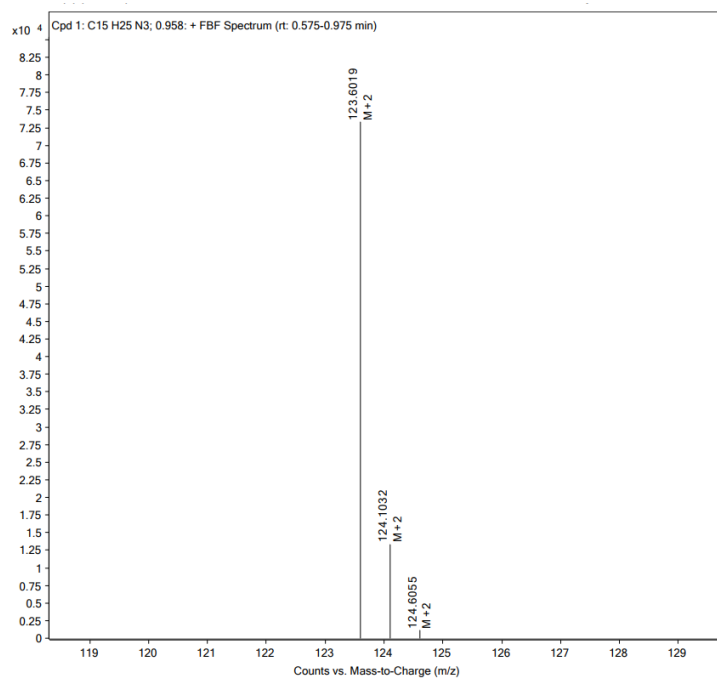


**Figure S55.** High-resolution mass spectrum of 1-(3-(4-methylpyridin-1-ium-1-yl)propyl)-1,4-diazabicyclo[2.2.2]octan-1-ium dibromide

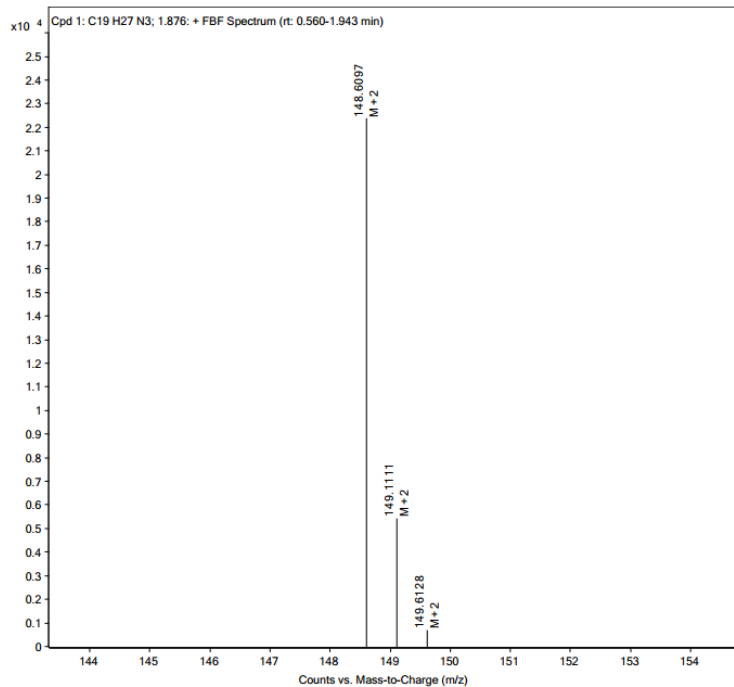


**Figure S56.** High-resolution mass spectrum of 1-(3-(4-methylquinolin-1-ium-1-yl)propyl)-1,4-diazabicyclo[2.2.2]octan-1-ium dibromide.

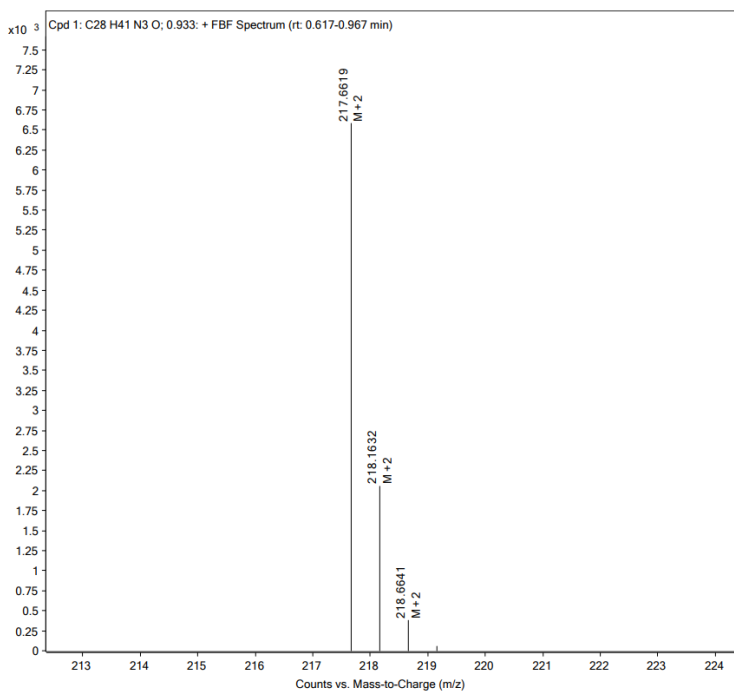


**Figure S57.** High-resolution mass spectrum of 1-(3-(4-(4-(hexyloxy)styryl)pyridin-1-ium-1-yl)propyl)-1,4-diazabicyclo[2.2.2]octan-1-ium dibromide (SPD-G)



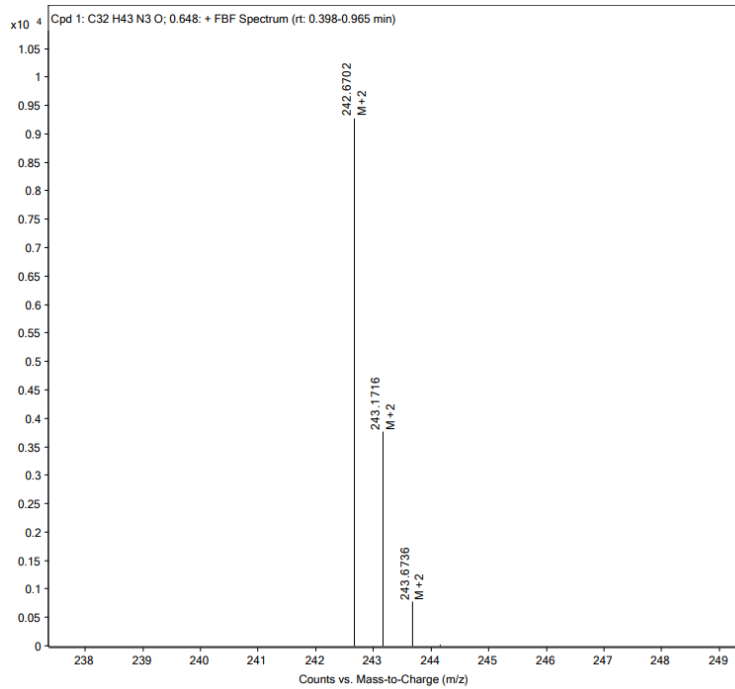


**Figure S58.** High-resolution mass spectrum of 1-(3-(4-(4-(dihexylamino)styryl)quinolin-1-ium-1-yl)propyl)-1,4-diazabicyclo[2.2.2]octan-1-ium dibromide (SQD-O)

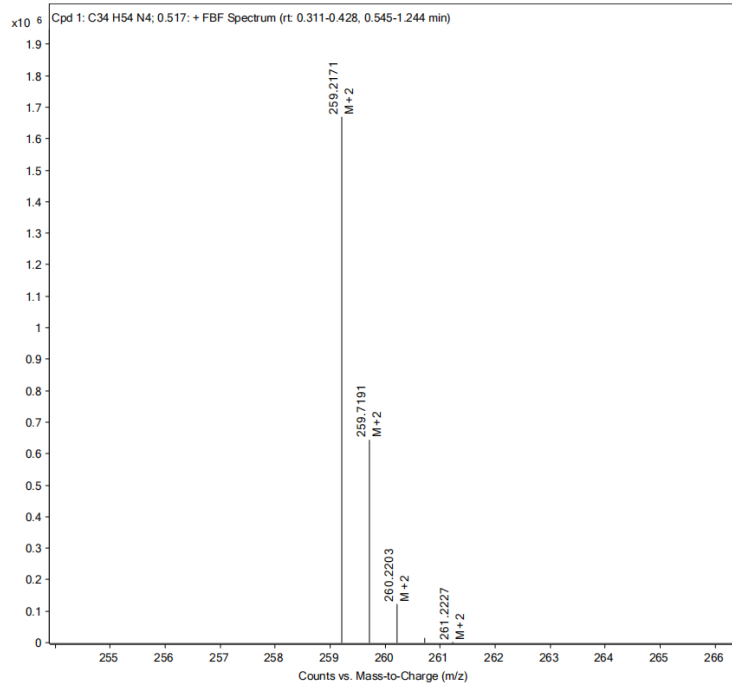


**Figure S59.** High-resolution mass spectrum of 1-(3-(4-(4-(hexyloxy)styryl)pyridin-1-ium-1-yl)propyl)-1,4-diazabicyclo[2.2.2]octan-1-ium dibromide (SPD-R)

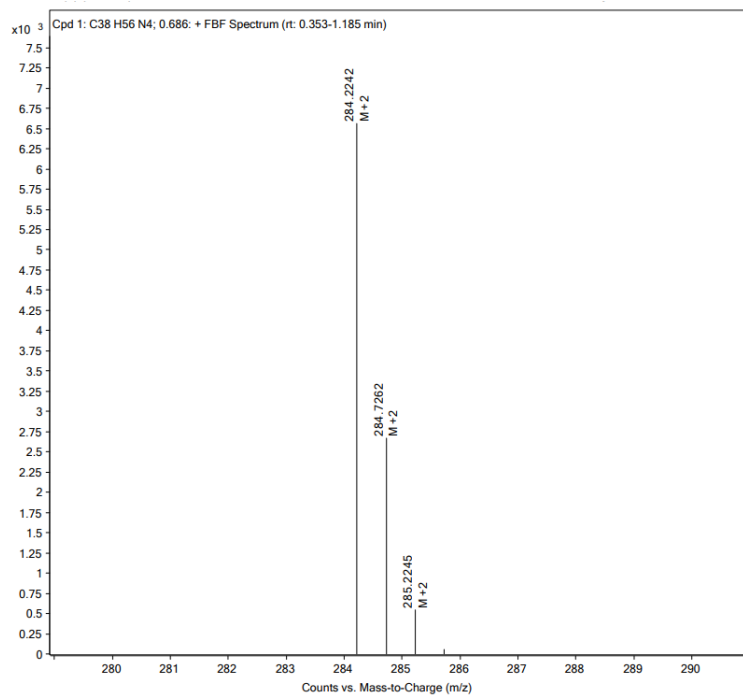


**Figure S60.** High-resolution mass spectrum of 1-(3-(4-(4-(dihexylamino)styryl)quinolin-1-ium-1-yl)propyl)-1,4-diazabicyclo[2.2.2]octan-1-ium bromide (SQD-NIR)